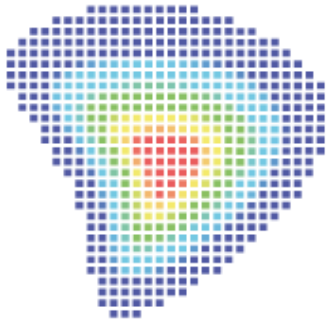

cniv 2017

2e Congrès National d'Imagerie du Vivant

8 > 9 novembre 2017 / Paris

AGENTS D'IMAGERIE
ONCOLOGIE NEUROSCIENCES
INFLAMMATOIRE-INFECTIEUX
CARDIOMÉTABOLISME
IMAGERIE INTERVENTIONNELLE

IMAGERIE NUCLÉAIRE
OPTIQUE RAYONS X
MEG/EEG IRM ULTRASONS
COUPLAGE DE MODALITÉS

*Nouvelles prises en charge des cancers*

# La médecine nucléaire pour l'évaluation thérapeutique : une avancée pour la prise en charge des cancers

## *Nuclear medicine for therapeutic evaluation: a breakthrough for the treatment of cancer*


**J Ph VUILLEZ**

*Responsable de la Clinique Universitaire de Médecine Nucléaire – Pôle d'Imagerie*
*CHU de Grenoble CS 10217 38043 Grenoble Cedex 9*
INSERM U-1039 Radiopharmaceutiques Biocliniques
Université Grenoble 1 - Site santé


Inserm
Institut national
de la santé et de la recherche médicale

CHU GRENOBLE ALPES
Centre Hospitalier Universitaire
Grenoble Alpes
CS 10217, 38043 Grenoble Cedex 9
04 76 76 75 75 - www.chu-grenoble.fr

UNIVERSITÉ Grenoble Alpes

# Cancer treatments

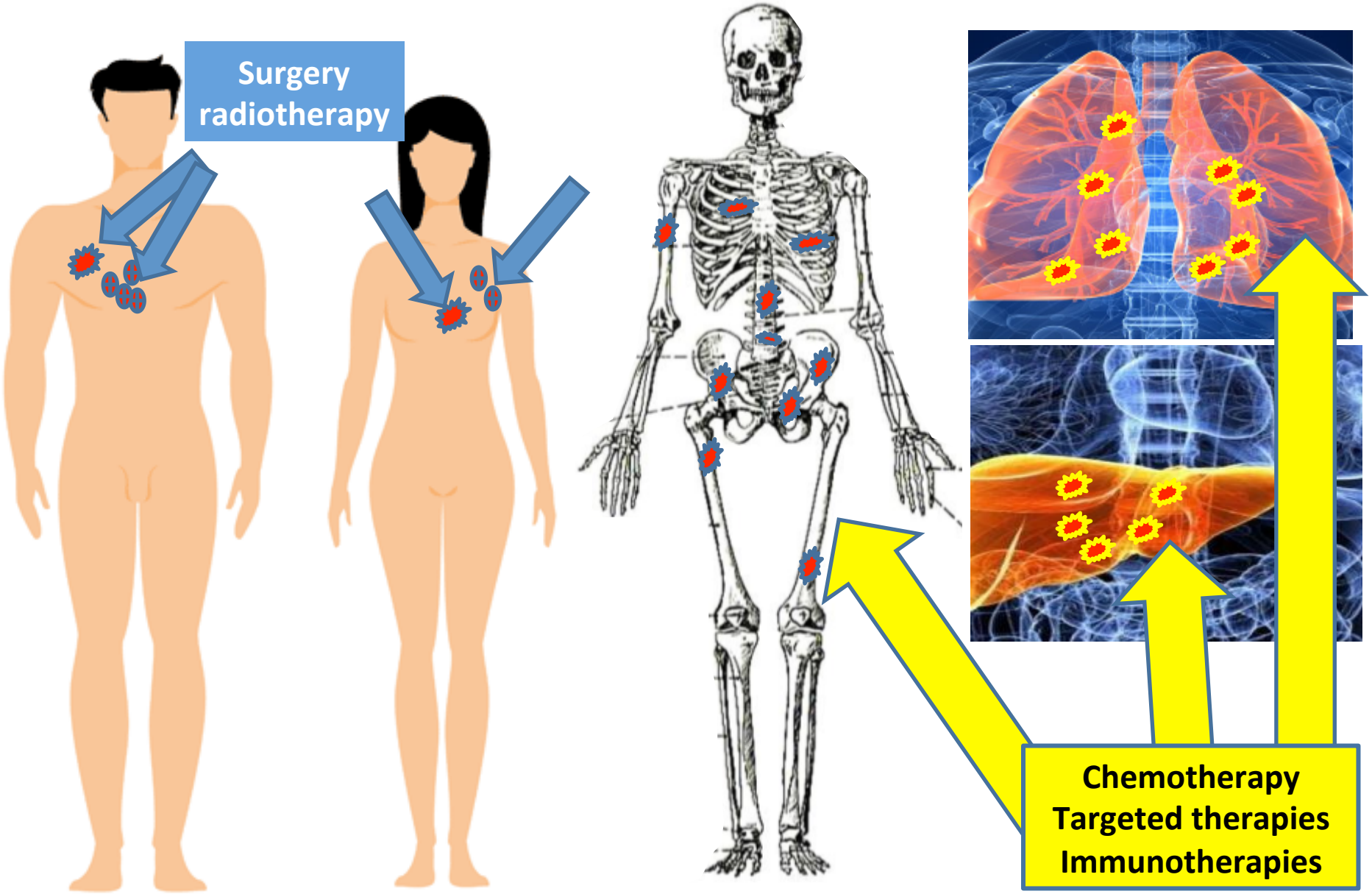

# Therapeutic evaluation

= Diagnosis of **residual disease**

- Locoregional
  - After surgery
  - After radiotherapy
- Systemic
  - After locoregional treatment: metastatic evolution?
  - **During systemic treatments: PREDICTION of response**
  - **At the end of systemic treatment: EVALUATION of response**

# Biomarkers = semiology

- Heart murmur: biomarker of valvulopathy
- Hyperglycemia: biomarker of diabetes

- PET-FDG scintigraphy : biomarker of disease extension/scalability…
- …

# Biomarker = physiopathology

- Heart murmur: turbulent flow
- Hyperglycemia: insulin deficiency

- FDG PET Scintigraphy: hyperconsumption of glucose by tumor cells

**Understanding the Warburg Effect: The Metabolic Requirements of Cell Proliferation**

Matthew G. Vander Heiden, *et al.*

*Science* **324**, 1029 (2009);

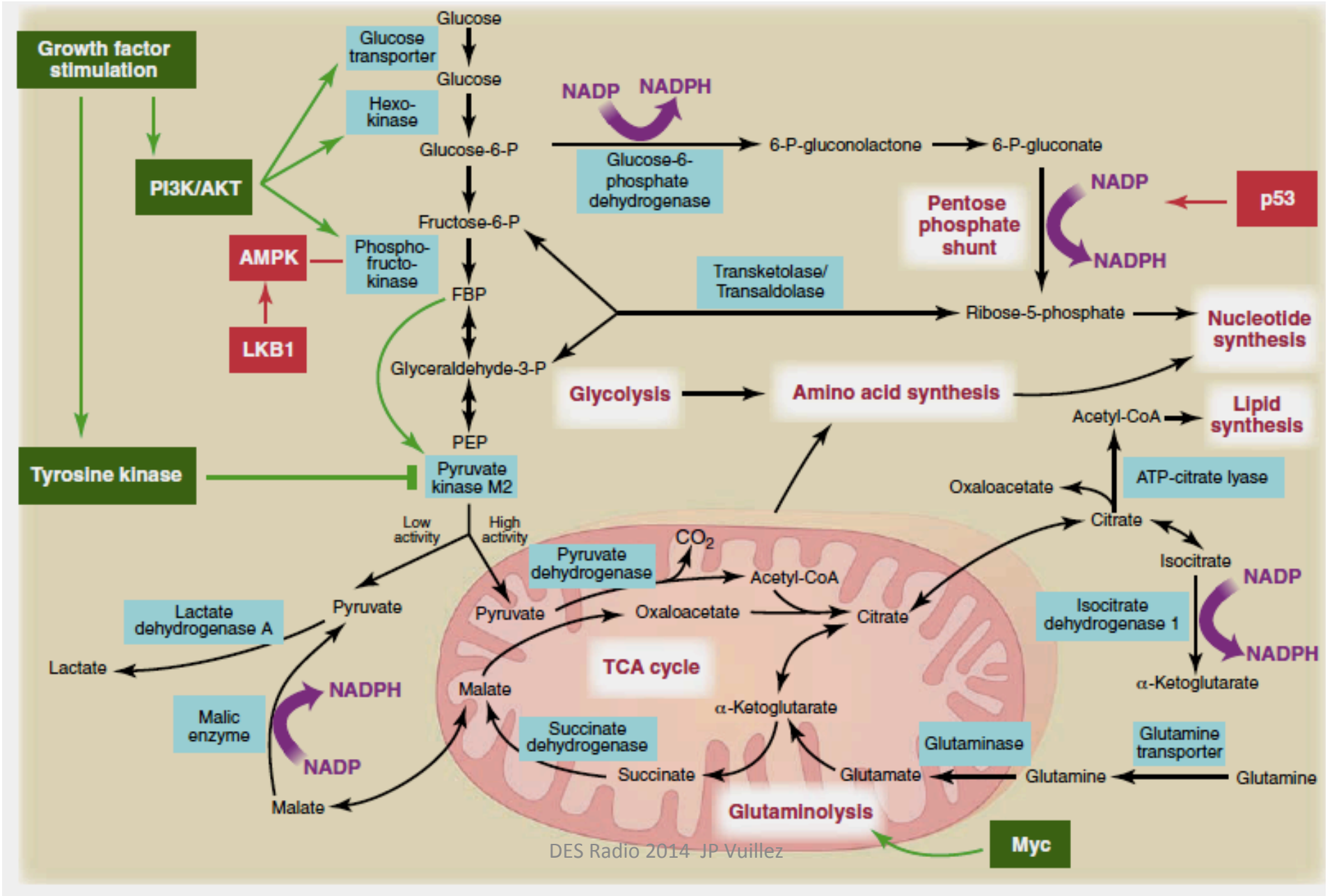

# Therapeutic evaluation: the example of malignant lymphomas

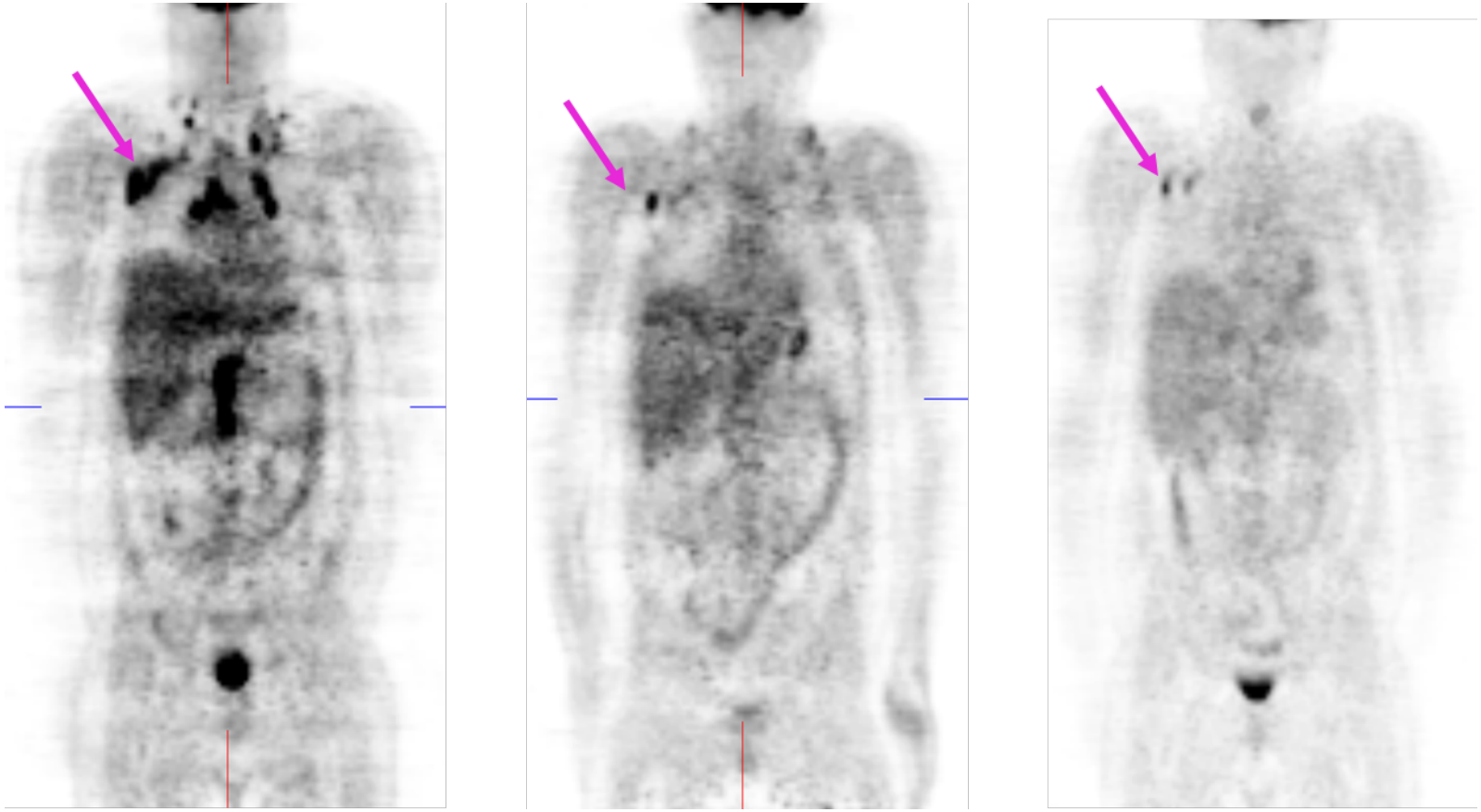

VOLUME 32 · NUMBER 27 · SEPTEMBER 20 2014

JOURNAL OF CLINICAL ONCOLOGY

SPECIAL ARTICLE

# Role of Imaging in the Staging and Response Assessment of Lymphoma: Consensus of the International Conference on Malignant Lymphomas Imaging Working Group

*Sally F. Barrington, N. George Mikhaeel, Lale Kostakoglu, Michel Meignan, Martin Hutchings, Stefan P. Müeller, Lawrence H. Schwartz, Emanuele Zucca, Richard I. Fisher, Judith Trotman, Otto S. Hoekstra, Rodney J. Hicks, Michael J. O'Doherty, Roland Hustinx, Alberto Biggi, and Bruce D. Cheson*

**Results**

A working paper was circulated for comment and presented at the Fourth International Workshop on PET in Lymphoma in Menton, France, and the 12th ICML in Lugano, Switzerland, to update the International Harmonisation Project guidance regarding PET. Recommendations were made to optimize the use of PET-CT in staging and response assessment of lymphoma, including qualitative and quantitative methods.

**Conclusion**

This article comprises the consensus reached to update guidance on the use of PET-CT for staging and response assessment for [$^{18}$F]fluorodeoxyglucose-avid lymphomas in clinical practice and late-phase trials.

**Table 1.** Summary of Recommendations

| Recommendations |
|---|
| Section 1: Interpretation of PET-CT scans |
| 1. Staging of FDG-avid lymphomas is recommended using visual assessment, with PET-CT images scaled to fixed SUV display and color table; focal uptake in HL and aggressive NHL is sensitive for bone marrow involvement and may obviate need for biopsy; MRI is modality of choice for suspected CNS lymphoma (type 1) |
| 2. Five-point scale is recommended for reporting PET-CT; results should be interpreted in context of anticipated prognosis, clinical findings, and other markers of response; scores 1 and 2 represent CMR; score 3 also probably represents CMR in patients receiving standard treatment (type 1) |
| 3. Score 4 or 5 with reduced uptake from baseline likely represents partial metabolic response, but at end of treatment represents residual metabolic disease; increase in FDG uptake to score 5, score 5 with no decrease in uptake, and new FDG-avid foci consistent with lymphoma represent treatment failure and/or progression (type 2) |
| Section 2: Role of PET-CT for staging |
| 1. PET-CT should be used for staging in clinical practice and clinical trials but is not routinely recommended in lymphomas with low FDG avidity; PET-CT may be used to select best site to biopsy (type 1) |
| 2. Contrast-enhanced CT when used at staging or restaging should ideally occur during single visit combined with PET-CT, if not already performed; baseline findings will determine whether contrast-enhanced PET-CT or lower-dose unenhanced PET-CT will suffice for additional imaging examinations (type 2) |
| 3. Bulk remains an important prognostic factor in some lymphomas; volumetric measurement of tumor bulk and total tumor burden, including methods combining metabolic activity and anatomical size or volume, should be explored as potential prognosticators (type 3) |
| Section 3: Role of interim PET |
| 1. If midtherapy imaging is performed, PET-CT is superior to CT alone to assess early response; trials are evaluating role of PET response–adapted therapy; currently, it is not recommended to change treatment solely on basis of interim PET-CT unless there is clear evidence of progression (type 1) |
| 2. Standardization of PET methods is mandatory for use of quantitative approaches and desirable for routine clinical practice (type 1) |
| 3. Data suggest that quantitative measures (eg, δSUVmax) could be used to improve on visual analysis for response assessment in DLBCL, but this requires further validation in clinical trials (type 2) |
| Section 4: Role of PET at end of treatment |
| 1. PET-CT is standard of care for remission assessment in FDG-avid lymphoma; in presence of residual metabolically active tissue, where salvage treatment is being considered, biopsy is recommended (type 1) |
| 2. Investigation of significance of PET-negative residual masses should be collected prospectively in clinical trials; residual mass size and location should be recorded on end-of-treatment PET-CT reports where possible (type 3) |
| 3. Emerging data support use of PET-CT after rituximab-containing chemotherapy in high–tumor burden FL; studies are warranted to confirm this finding in patients receiving maintenance therapy (type 2) |
| 4. Assessment with PET-CT could be used to guide decisions before high-dose chemotherapy and ASCT, but additional studies are warranted (type 3) |

Abbreviations: ASCT, autologous stem-cell transplantation; CMR, complete metabolic response; CT, computed tomography; DLBCL, diffuse large B-cell lymphoma; FDG, [$^{18}$F]fluorodeoxyglucose; FL, follicular lymphoma; HL, Hodgkin lymphoma; MRI, magnetic resonance imaging; NHL, non-Hodgkin lymphoma; PET, positron emission tomography; SUV, standardized uptake value; δSUVmax, change in maximum SUV.

**Table 2.** FDG Avidity According to WHO Classification

| Histology | No. of Patients | FDG Avid (%) |
|---|---|---|
| HL | 489 | 97-100 |
| DLBCL | 446 | 97-100 |
| FL | 622 | 91-100 |
| Mantle-cell lymphoma | 83 | 100 |
| Burkitt's lymphoma | 24 | 100 |
| Marginal zone lymphoma, nodal | 14 | 100 |
| Lymphoblastic lymphoma | 6 | 100 |
| Anaplastic large T-cell lymphoma | 37 | 94-100* |
| NK/T-cell lymphoma | 80 | 83-100 |
| Angioimmunoblastic T-cell lymphoma | 31 | 78-100 |
| Peripheral T-cell lymphoma | 93 | 86-98 |
| MALT marginal zone lymphoma | 227 | 54-81 |
| Small lymphocytic lymphoma | 49 | 47-83 |
| Enteropathy-type T-cell lymphoma | 20 | 67-100 |
| Marginal zone lymphoma, splenic | 13 | 53-67 |
| Marginal zone lymphoma, unspecified | 12 | 67 |
| Mycosis fungoides | 24 | 83-100 |
| Sezary syndrome | 8 | 100† |
| Primary cutaneous anaplastic large T-cell lymphoma | 14 | 40-60 |
| Lymphomatoid papulosis | 2 | 50 |
| Subcutaneous panniculitis-like T-cell lymphoma | 7 | 71 |
| Cutaneous B-cell lymphoma | 2 | 0 |

NOTE. Data adapted,[64] with additional updates.[18,33,34,65-67]

Abbreviations: DLBCL, diffuse large B-cell lymphoma; FDG, [$^{18}$F]fluorodeoxyglucose; FL, follicular lymphoma; HL, Hodgkin lymphoma; MALT, mucosa-associated lymphoid tissue; NK, natural killer.

*Only 27% of cutaneous sites.

†Only 62% of cutaneous sites.

**Table 1** The Deauville five point scale. The scale scores the most intense uptake in a site of initial disease, if present

| Score | Definition |
|---|---|
| 1 | No uptake |
| 2 | Uptake ≤ mediastinum |
| 3 | Uptake > mediastinum but ≤ liver |
| 4 | Moderately increased uptake compared to the liver |
| 5 | Markedly increased uptake compared to the liver and/or new lesions |
| X | New areas of uptake unlikely to be related to lymphoma |

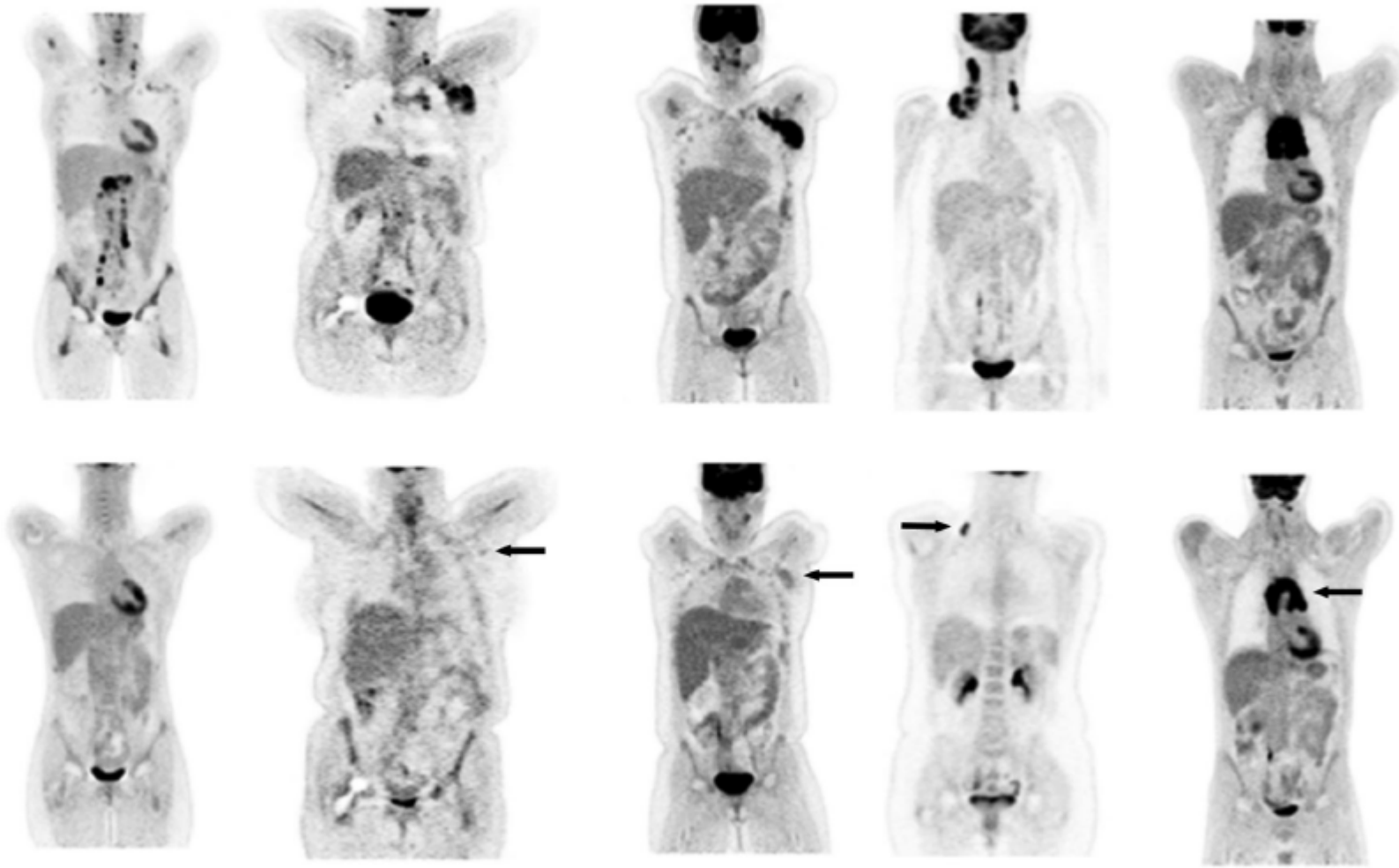

**Fig. 1** Coronal slices of PET images in patients at staging and at response with different grades of FDG uptake, from *left to right* corresponding to Deauville score 1–5

*Bilan d'extension d'un lymphome de Hodgkin de localisation médiastinale*

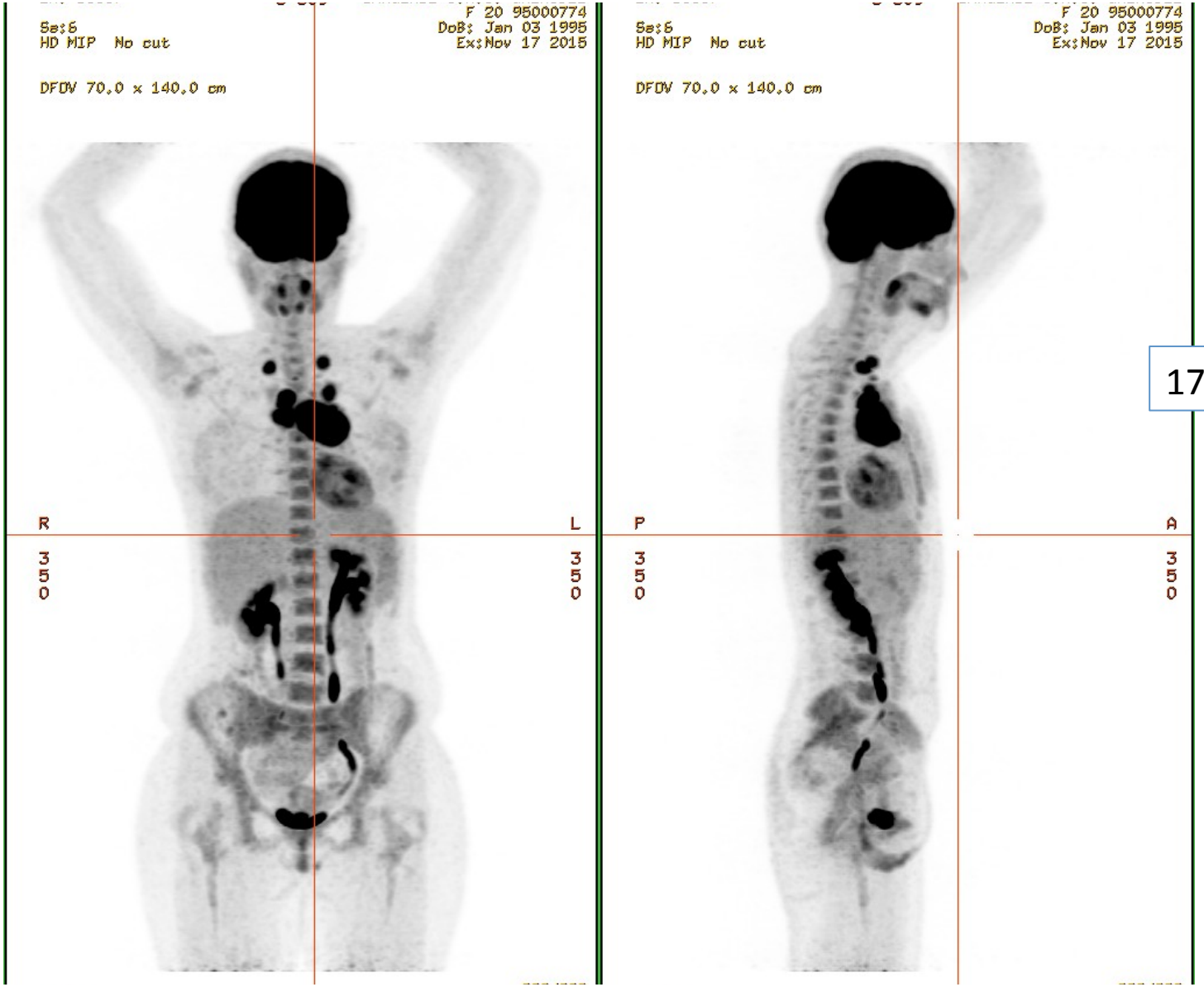


17 nov 2015

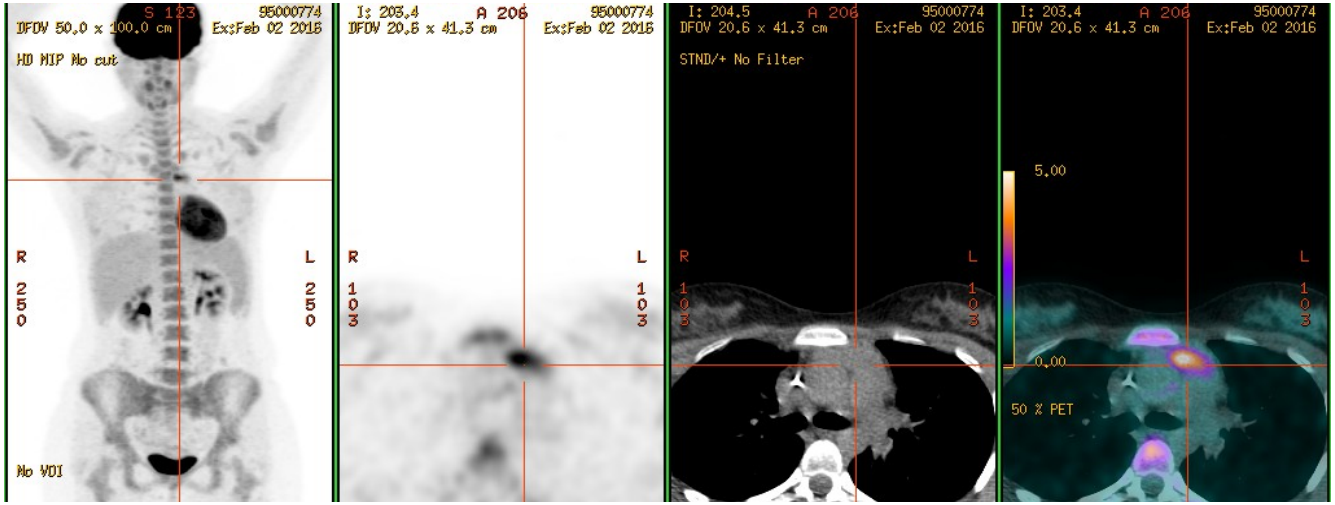


2 février 2016
(2,5 mois)

**Réponse métabolique partielle après deux cures de chimiothérapie, avec persistance d'une masse ganglionnaire toujours intensément hypermétabolique au niveau médiastinal antérieur gauche (Deauville 5)**

17 nov 2015

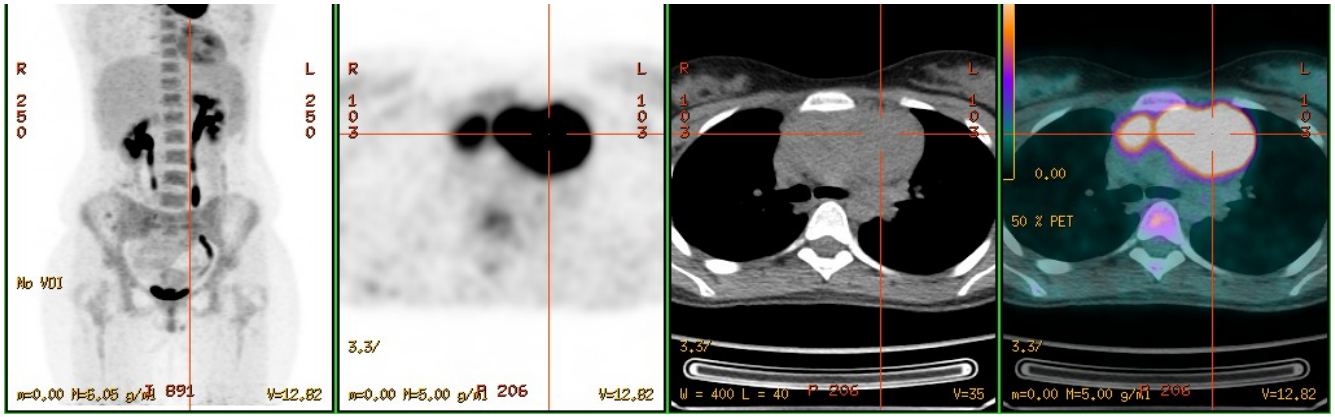

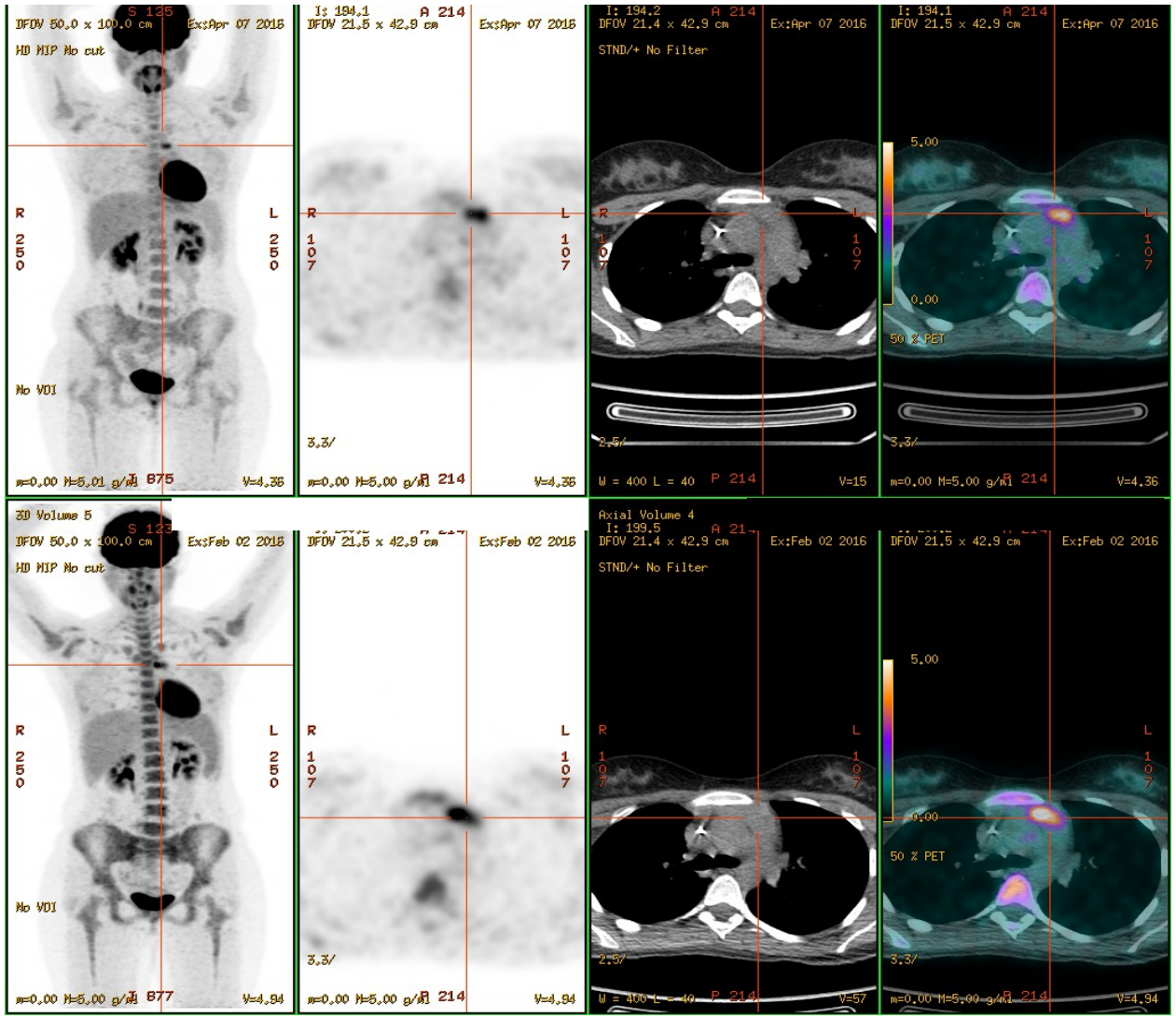


7 avril 2016
(6 mois)

FIN DE TTT

2 février 2016
(2,5 mois)

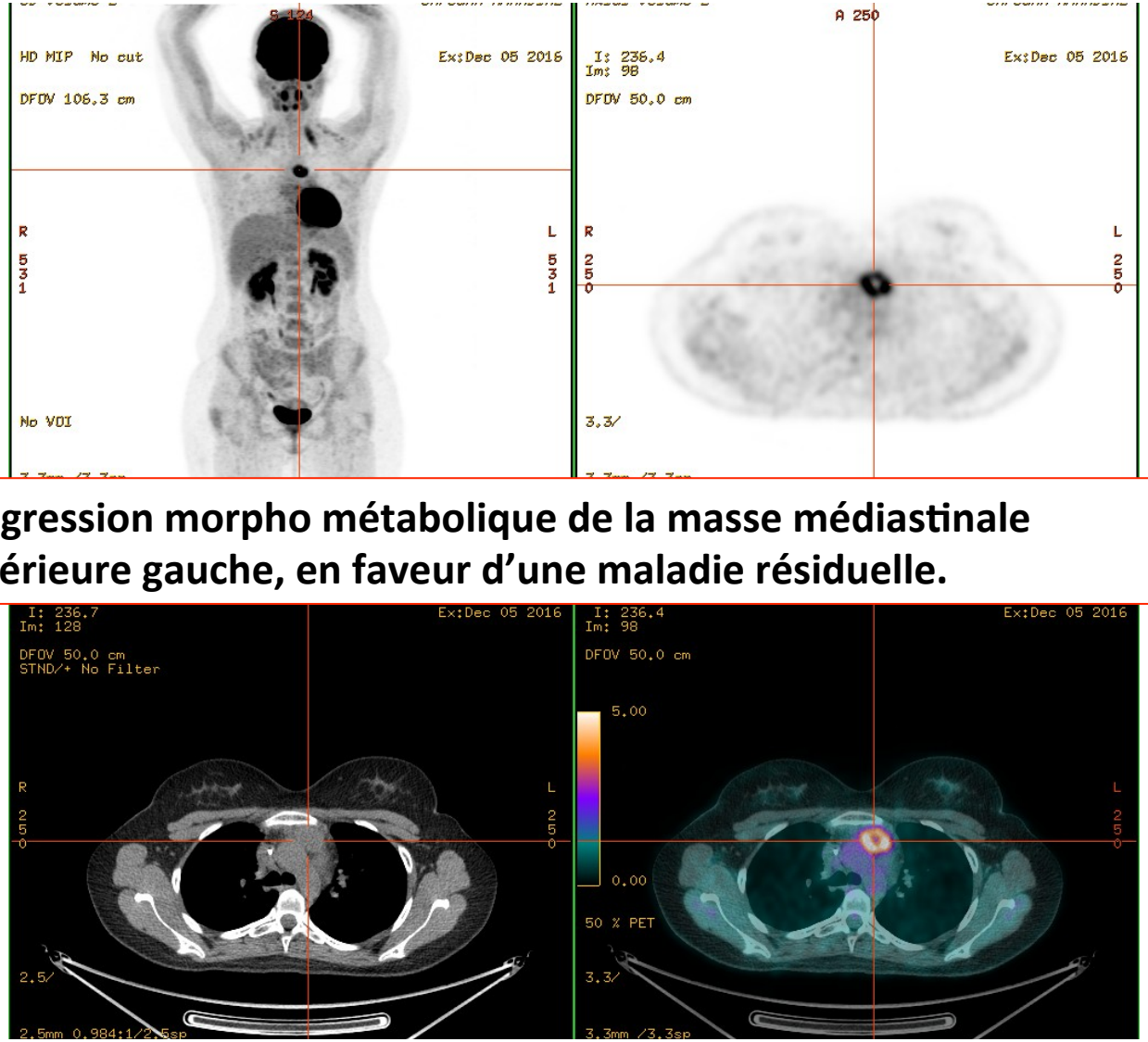


5 décembre 2016
(11 mois)

**Progression morpho métabolique de la masse médiastinale antérieure gauche, en faveur d'une maladie résiduelle.**

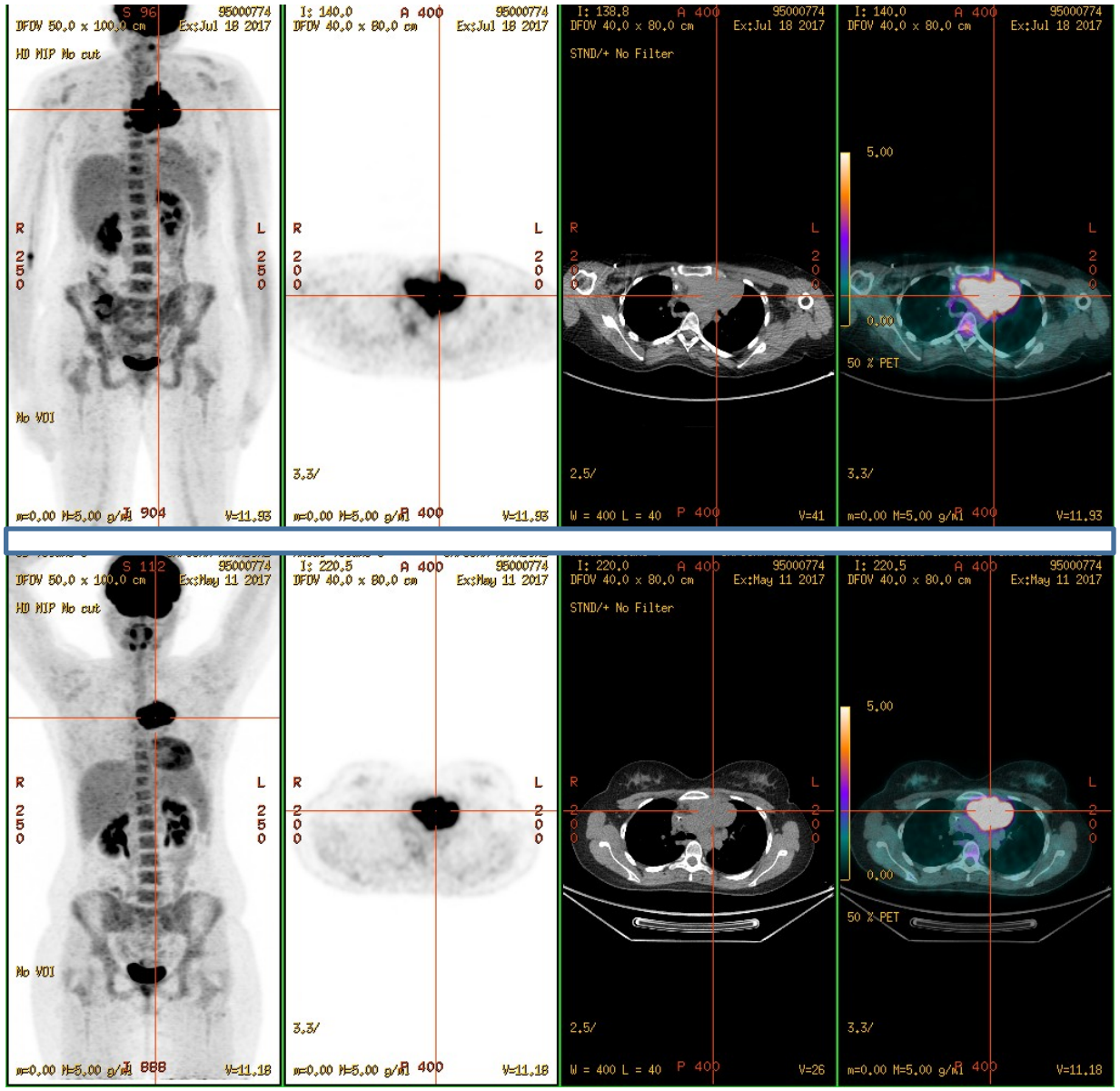


18 juillet 2017
(20 mois)

11 mai 2017
(18 mois)

# Solid tumours

Wahl RL, Jacene H, Kasamon Y, et al. From RECIST to PERCIST: evolving considerations for PET response criteria in solid tumors. J Nucl Med. 2009;50(Suppl 1):122S–5S.

**TABLE 7.** Comparison of EORTC and PERCIST 1.0 (*36*)

| Characteristic | EORTC | PERCIST 1.0 |
|---|---|---|
| Measurability of lesions at baseline | 1. Tumor regions defined on pretreatment scan should be drawn on region of high $^{18}$F-FDG uptake representing viable tumor. Whole tumor uptake should also be recorded.<br>2. Same ROI volumes should be sampled on subsequent scans and positioned as close to original tumor volume as possible. Coregistration method should be recorded.<br>3. Uptake measurements should be made for mean and maximal tumor ROI counts per pixel per second calibrated as MBq/L.<br>4. Alterations in extent of $^{18}$F-FDG uptake should be documented, i.e., increase in orthogonal tumor dimensions including longest tumor dimension.<br>5. Partial volume may affect measurement of $^{18}$F-FDG uptake. Tumor size from anatomic imaging in relation to PET scanner resolution should be documented where possible. | 1. Measurable target lesion is hottest single tumor lesion SUL of "maximal 1.2-cm diameter volume ROI in tumor" (SUL peak). SUL peak is at least 1.5-fold greater than liver SUL mean + 2 SDs (in 3-cm spherical ROI in normal right lobe of liver). If liver is abnormal, primary tumor should have uptake $> 2.0 \times$ SUL mean of blood pool in 1-cm-diameter ROI in descending thoracic aorta extended over 2-cm *z*-axis.<br>2. Tumor with maximal SUL peak is assessed after treatment. Although typically this is in same region of tumor as that with highest SUL peak at baseline, it need not be.<br>3. Uptake measurements should be made for peak and maximal single-voxel tumor SUL. Other SUV metrics, including SUL mean at 50% or 70% of SUV peak, can be collected as exploratory data; TLG can be collected ideally on basis of voxels more intense than 2 SDs above liver mean SUL (see below).<br>4. These parameters can be recorded as exploratory data on up to 5 measurable target lesions, typically the 5 hottest lesions, which are typically the largest, and no more than 2 per organ. Tumor size of these lesions can be determined per RECIST 1.1. |
| Normalization of uptake | Scanners should provide reproducible data. Reporting would need to be accompanied by adequate and disclosed reproducibility measurements from each center. An empiric 25% was found to be a useful cutoff point, but reproducibility analysis is needed to determine appropriate cutoffs for statistical significance. | Normal liver SUL must be within 20% (and $<$0.3 SUL mean units) for baseline and follow-up study to be assessable. If liver is abnormal, blood-pool SUL must be within 20% (and $<$0.3 SUL mean units) for baseline and follow-up study to be assessable. Uptake time of baseline study and follow-up study 2 must be within 15 min of each other to be assessable. Typically, these are at mean of 60 min after injection but no less than 50 min after injection. Same scanner, or same scanner model at same site, injected dose, acquisition protocol (2- vs. 3-dimensional), and software for reconstruction, should be used. Scanners should provide reproducible data and be properly calibrated. |
| Objective response | CMR: complete resolution of $^{18}$F-FDG uptake within tumor volume so that it was indistinguishable from surrounding normal tissue. | CMR: complete resolution of $^{18}$F-FDG uptake within measurable target lesion so that it is less than mean liver activity and indistinguishable from surrounding background blood-pool levels. Disappearance of all other lesions to background blood-pool levels. Percentage decline in SUL should be recorded from measurable region, as well as (ideally) time in weeks after treatment was begun (i.e., CMR $-$90, 4). No new $^{18}$F-FDG–avid lesions in pattern typical of cancer. If progression by RECIST, must verify with follow-up. |

Journal of Nuclear Medicine, published on October 19, 2017 as doi:10.2967/jnumed.117.197988

# Appropriate Use Criteria for $^{18}$F-FDG PET/CT in Restaging and Treatment Response Assessment of Malignant Disease

Hossein Jadvar[1], Patrick M. Colletti[4], Roberto Delgado-Bolton[2], Giuseppe Esposito[1], Bernd J. Krause[2], Andrei H. Iagaru[1], Helen Nadel[1,5,6], David I. Quinn[3], Eric Rohren[1], Rathan M. Subramaniam[4], Katherine Zukotynski[1], Julie Kauffman[1], Sukhjeet Ahuja[1], and Landis Griffeth[1]

Two reviewers independently assessed abstracts and full-text articles for inclusion and rated study quality as defined by the established PICOTS parameters. The quality (based on risk of bias) for each study was categorized as "good," "fair," or "poor" by using the predefined criteria for each study design. Specifically, Quality Assessment of Diagnostic Accuracy Studies-2 (QUADAS-2) was used for diagnostic accuracy studies (*4*) and Assessment of Multiple Systematic Reviews (AMSTAR) for systematic reviews (*5*). The strength of overall evidence was graded as high, moderate, low, or very low by using GRADE methods, which were based on quality of evidence, consistency, directness, precision, and reporting bias.

Literature searches resulted in 2,665 potentially relevant articles. After dual review of abstracts and titles, 1,120 articles were selected for full-text dual review and 45 studies were determined to meet inclusion criteria and included in this review.

**TABLE 1**
Clinical Scenarios for Breast Cancer

| Scenario no. | Description | Appropriateness | Score |
|---|---|---|---|
| 1 | Restaging for detection of local recurrence | Appropriate | 8 |
| 2 | Restaging for detection of metastases | Appropriate | 7 |
| 3 | Treatment response evaluation | Appropriate | 7 |

**TABLE 3**
Clinical Scenarios for Lymphoma

| Scenario no. | Description | Appropriateness | Score |
|---|---|---|---|
| 1 | Detection of recurrent disease | Appropriate | 8 |
| 2 | Treatment response evaluation | Appropriate | 9 |

**TABLE 2**
Clinical Scenarios for Colorectal Cancer

| Scenario no. | Description | Appropriateness | Score |
|---|---|---|---|
| 1 | Restaging for detection of local recurrence | Appropriate | 7 |
| 2 | Restaging for detection of metastases | Appropriate | 8 |
| 3 | Detection of local recurrence or metastasis in the case of rising tumor markers with negative or equivocal first-line imaging (e.g., contrast-enhanced CT or MRI) | Appropriate | 8 |
| 4 | Treatment response evaluation | May be Appropriate | 6 |
| 5 | Assessment of response of metastases after chemotherapy | May be appropriate | 6 |
| 6 | Early assessment of metastases during chemotherapy | May be appropriate | 6 |
| 7 | Assessment of efficacy of neoadjuvant therapy for advanced rectal carcinoma | May be appropriate | 6 |
| 8 | Assessment of efficacy of localized minimally invasive therapy | May be appropriate | 6 |

**TABLE 4**
Clinical Scenarios for Lung Cancer

| Scenario no. | Description | Appropriateness | Score |
|---|---|---|---|
| 1 | Restaging for detection of local recurrence | Appropriate | 7 |
| 2 | Restaging for detection of metastases | Appropriate | 7 |
| 3 | Treatment response evaluation | Appropriate | 7 |

**TABLE 5**
Clinical Scenarios for Melanoma

| Scenario no. | Description | Appropriateness | Score |
|---|---|---|---|
| 1 | Restaging for detection of recurrent disease | Appropriate | 9 |
| 2 | Treatment response evaluation | Appropriate | 7 |

**TABLE 6**
Clinical Scenarios for Sarcoma

| Scenario no. | Description | Appropriateness | Score |
|---|---|---|---|
| 1 | Restaging for detection of local recurrence | Appropriate | 7 |
| 2 | Restaging for detection of metastases | Appropriate | 7 |
| 3 | Treatment response evaluation | Appropriate | 8 |

**TABLE 7**
Clinical Scenarios for Head and Neck Cancer

| Scenario no. | Description | Appropriateness | Score |
|---|---|---|---|
| 1 | Restaging for detection of local recurrence | Appropriate | 7 |
| 2 | Restaging for detection of metastases | Appropriate | 9 |
| 3 | Treatment response evaluation | Appropriate | 7 |

Eur J Nucl Med Mol Imaging
DOI 10.1007/s00259-017-3836-8

Published online: 22 September 2017

ORIGINAL ARTICLE

# The role of interim FDG PET-CT after induction chemotherapy as a predictor of concurrent chemoradiotherapy efficacy and prognosis for head and neck cancer

Ka-Rham Kim[1] · Hyun-Jeong Shim[1] · Jun-Eul Hwang[1] · Sang-Hee Cho[1] · Ik-Joo Chung[1] · Ki Seong Park[2] · Sae-Ryung Kang[2] · Seong Young Kwon[2] · Woong-Ki Chung[3] · Woo Kyun Bae[1,4]

43 patients

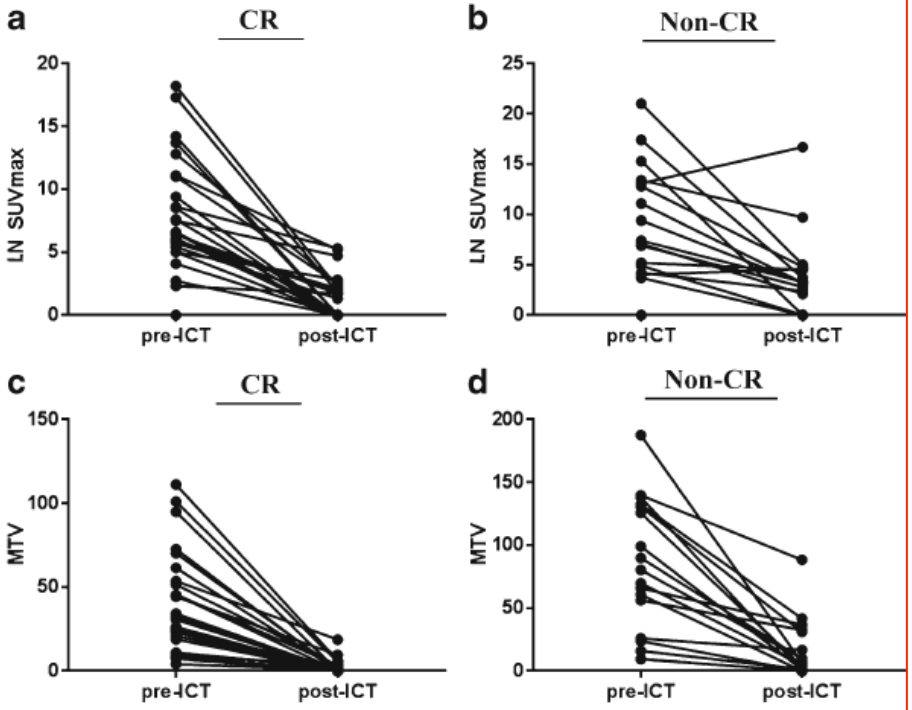


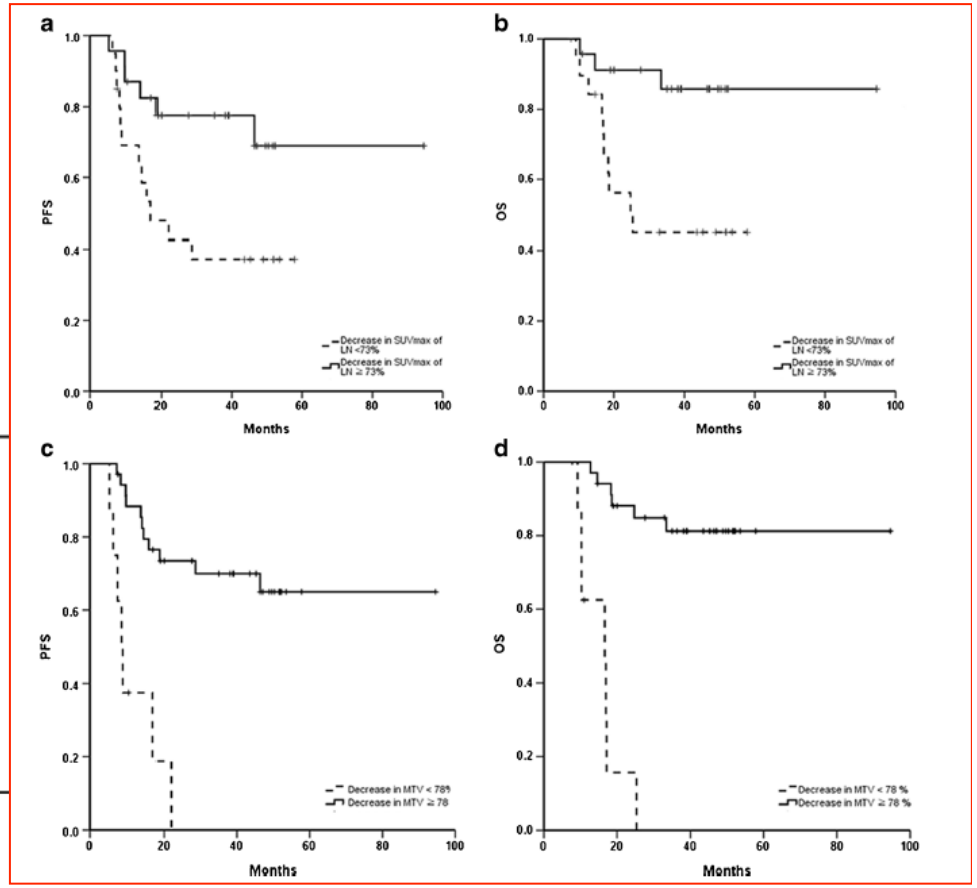

# Powerful Prognostic Stratification By [$^{18}$F]Fluorodeoxyglucose Positron Emission Tomography in Patients With Metastatic Breast Cancer Treated With High-Dose Chemotherapy

*Florent Cachin, H. Miles Prince, Annette Hogg, Robert E. Ware, and Rodney J. Hicks*

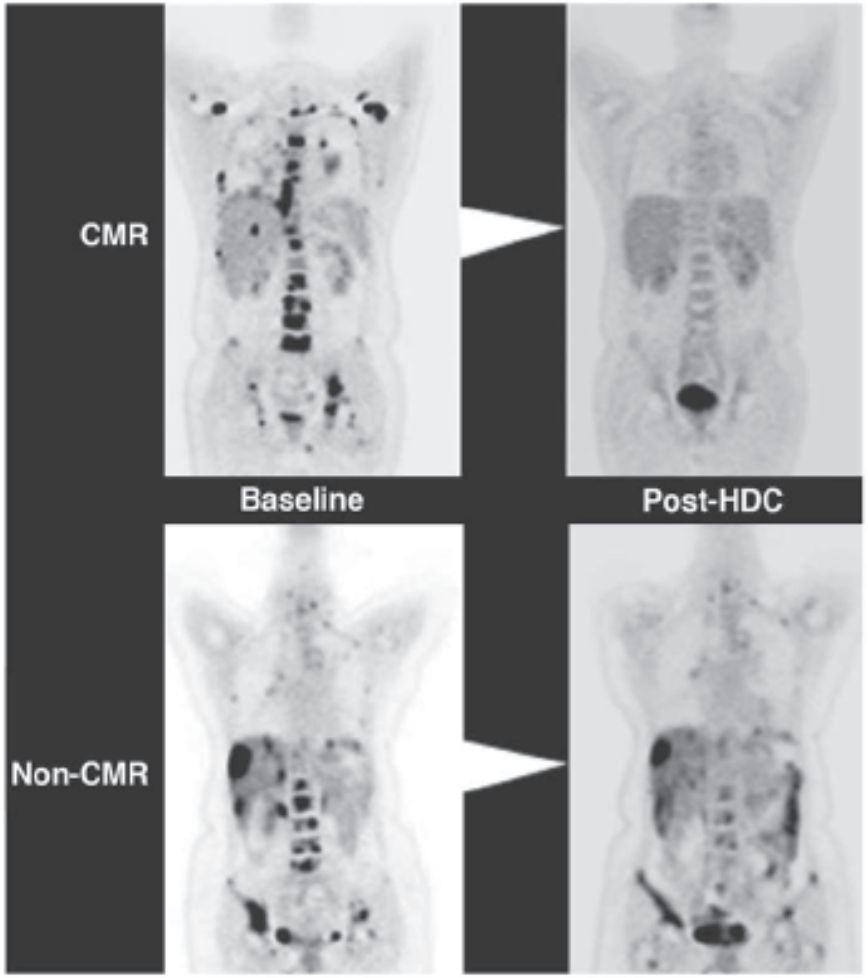


JOURNAL OF CLINICAL ONCOLOGY

VOLUME 24 · NUMBER 19 · JULY 1 2006

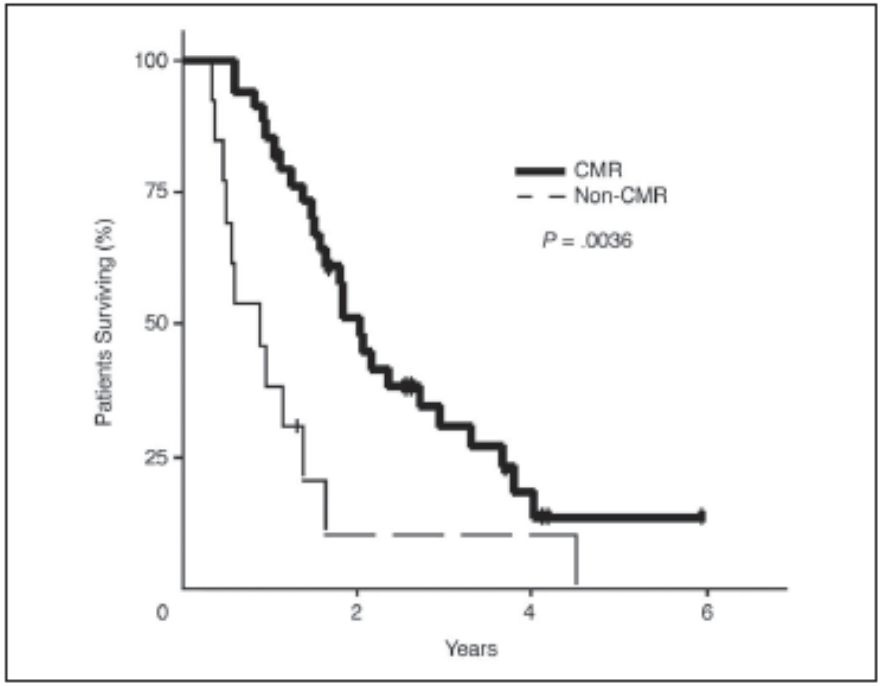

# Hallmarks of Cancer: The Next Generation

Douglas Hanahan[1,2,*] and Robert A. Weinberg[3,*]

646 Cell *144*, March 4, 2011 ©2011 Elsevier Inc.

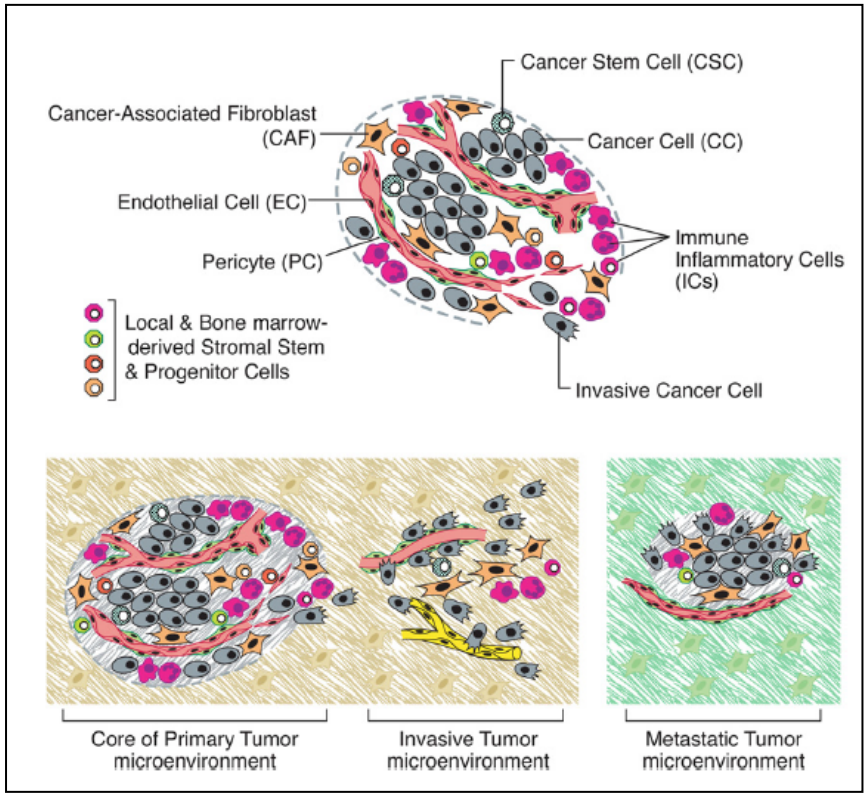


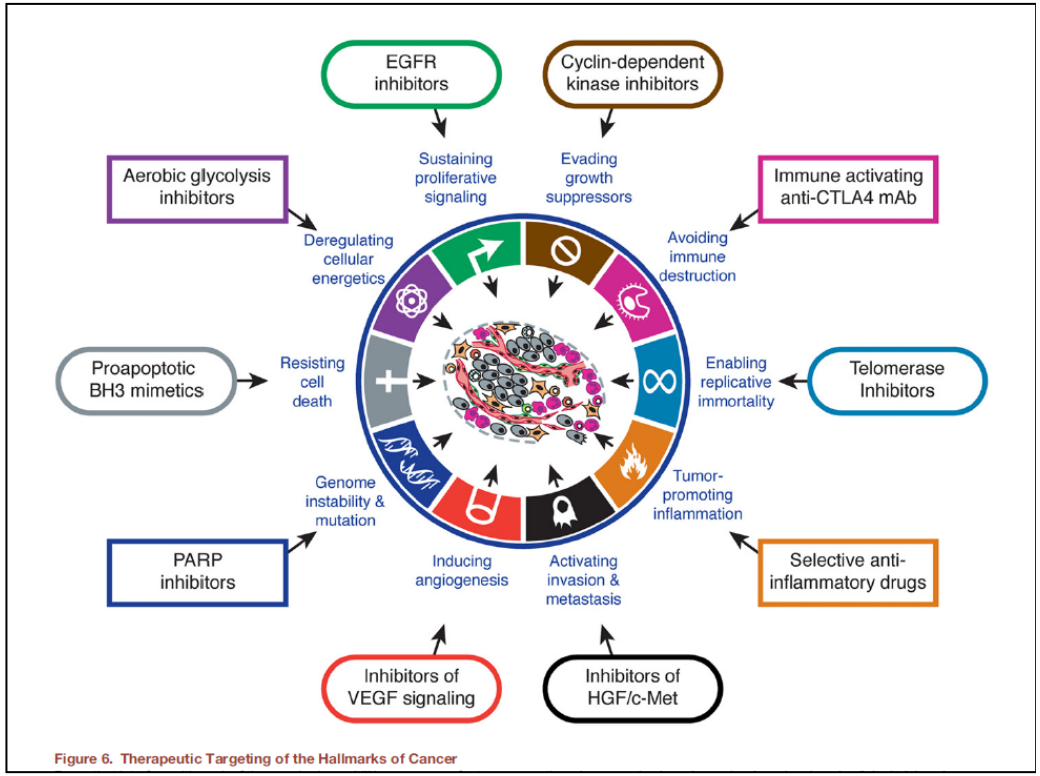


Figure 6. Therapeutic Targeting of the Hallmarks of Cancer

# Hallmarks of Cancer: The Next Generation

Douglas Hanahan[1,2,*] and Robert A. Weinberg[3,*]

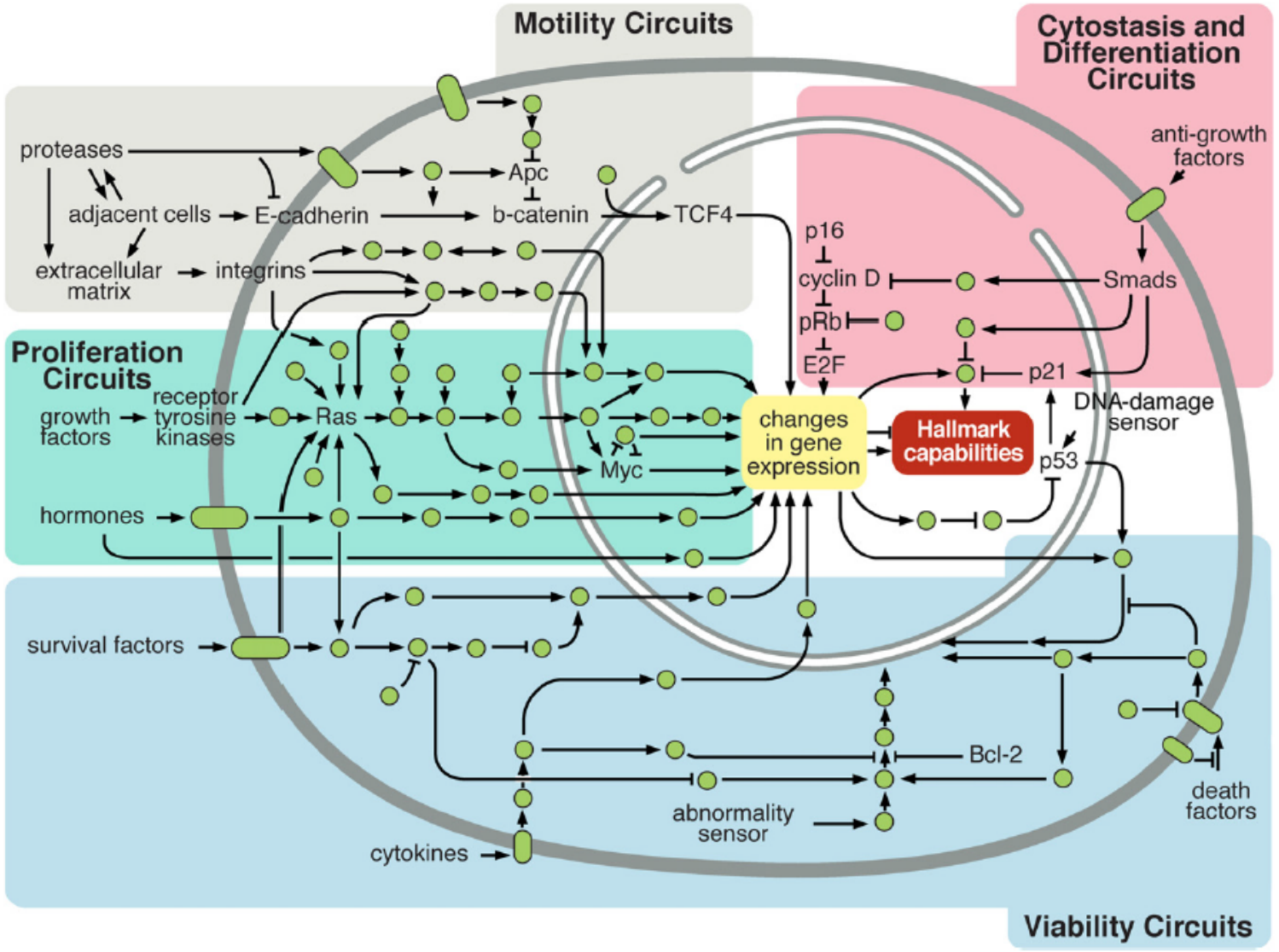


**Figure 2. Intracellular Signaling Networks Regulate the Operations of the Cancer Cell**

An elaborate integrated circuit operates within normal cells and is reprogrammed to regulate hallmark capabilities within cancer cells. Separate subcircuits, depicted here in differently colored fields, are specialized to orchestrate the various capabilities. At one level, this depiction is simplistic, as there is considerable crosstalk between such subcircuits. In addition, because each cancer cell is exposed to a complex mixture of signals from its microenvironment, each of these subcircuits is connected with signals originating from other cells in the tumor microenvironment, as outlined in Figure 5.

# Hallmarks of Cancer: The Next Generation

Douglas Hanahan[1,2,*] and Robert A. Weinberg[3,*]

646 Cell *144*, March 4, 2011 ©2011 Elsevier Inc.

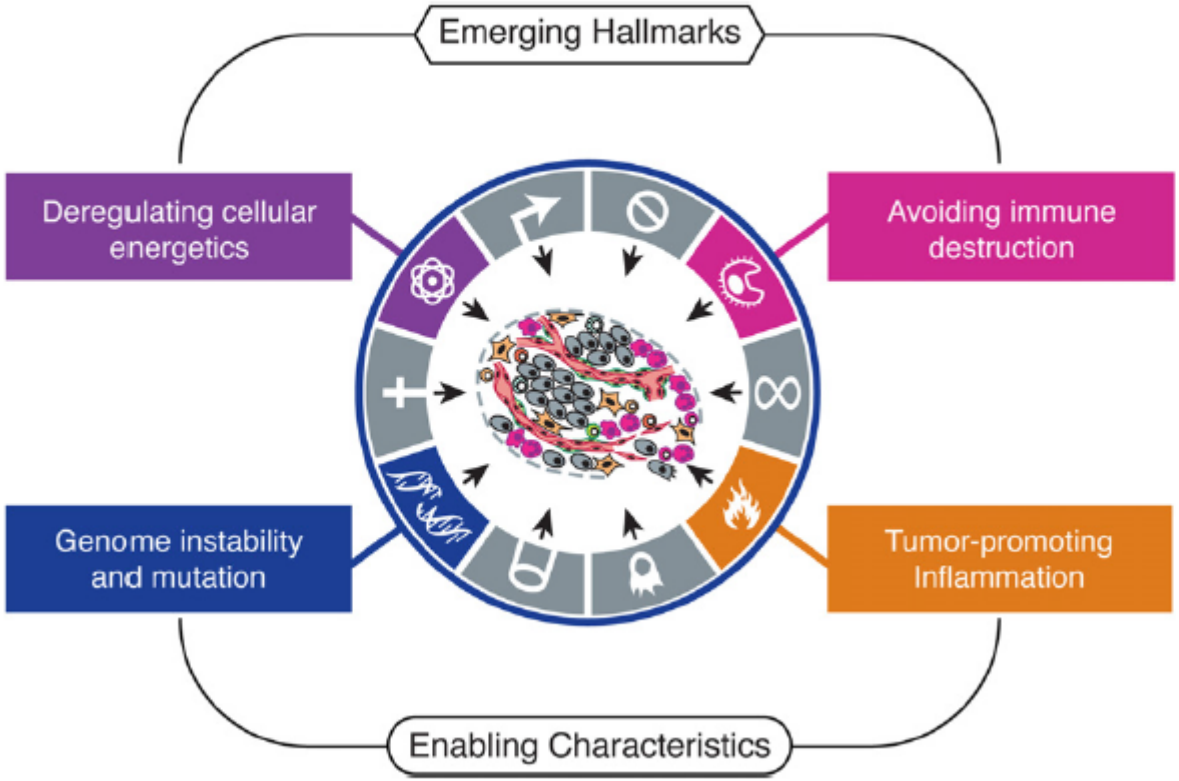


**Figure 3. Emerging Hallmarks and Enabling Characteristics**

An increasing body of research suggests that two additional hallmarks of cancer are involved in the pathogenesis of some and perhaps all cancers. One involves the capability to modify, or reprogram, cellular metabolism in order to most effectively support neoplastic proliferation. The second allows cancer cells to evade immunological destruction, in particular by T and B lymphocytes, macrophages, and natural killer cells. Because neither capability is yet generalized and fully validated, they are labeled as emerging hallmarks. Additionally, two consequential characteristics of neoplasia facilitate acquisition of both core and emerging hallmarks. Genomic instability and thus mutability endow cancer cells with genetic alterations that drive tumor progression. Inflammation by innate immune cells designed to fight infections and heal wounds can instead result in their inadvertent support of multiple hallmark capabilities, thereby manifesting the now widely appreciated tumor-promoting consequences of inflammatory responses.

# Hallmarks of Cancer: The Next Generation

Douglas Hanahan[1,2,*] and Robert A. Weinberg[3,*]

646 Cell *144*, March 4, 2011 ©2011 Elsevier Inc.

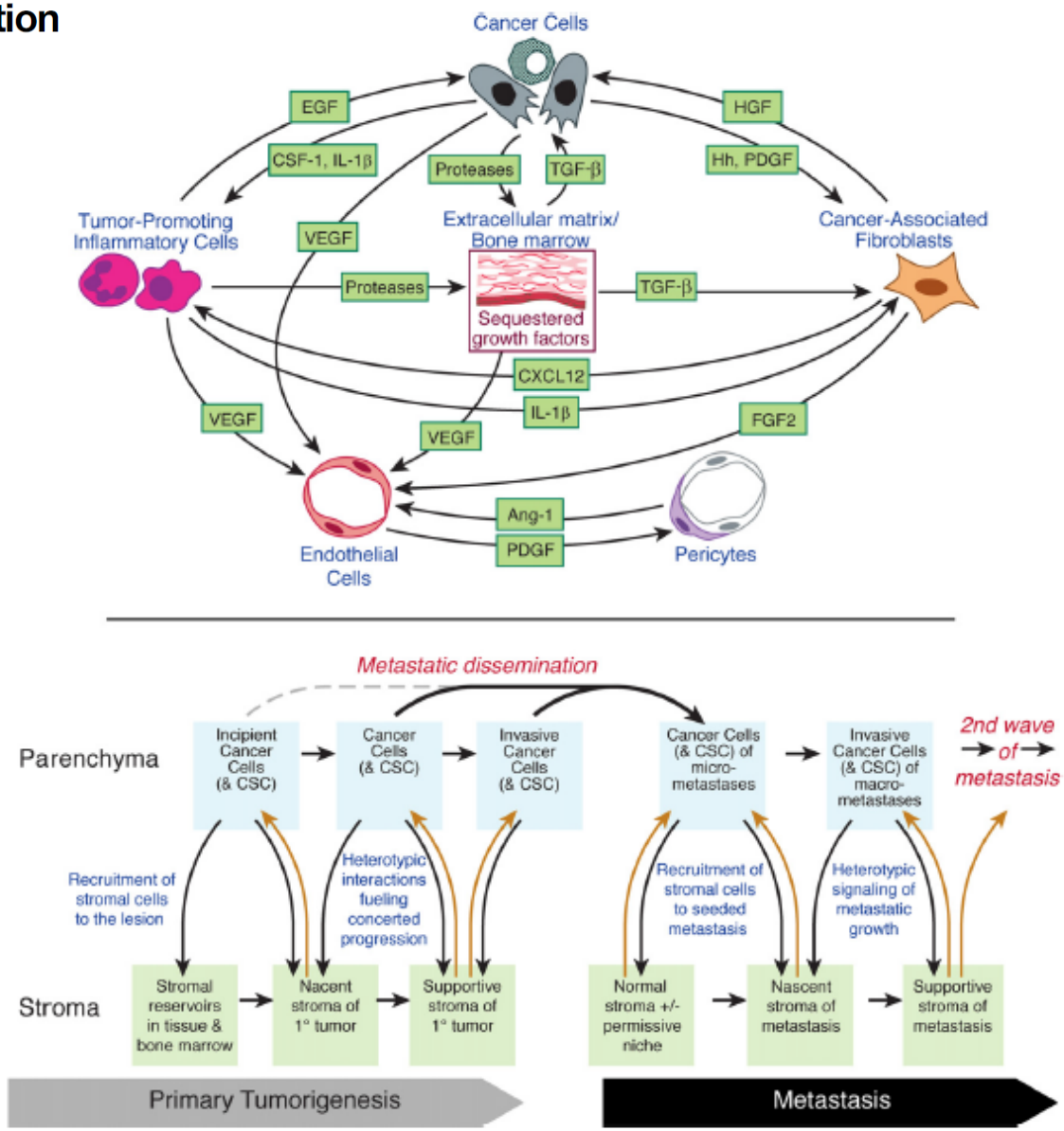


**Figure 5. Signaling Interactions in the Tumor Microenvironment during Malignant Progression**

(Upper) The assembly and collective contributions of the assorted cell types constituting the tumor microenvironment are orchestrated and maintained by reciprocal heterotypic signaling interactions, of which only a few are illustrated.

(Lower) The intracellular signaling depicted in the upper panel within the tumor microenvironment is not static but instead changes during tumor progression as a result of reciprocal signaling interactions between cancer cells of the parenchyma and stromal cells that convey the increasingly aggressive phenotypes that underlie growth, invasion, and metastatic dissemination. Importantly, the predisposition to spawn metastatic lesions can begin early, being influenced by the differentiation program of the normal cell-of-origin or by initiating oncogenic lesions. Certain organ sites (sometimes referred to as "fertile soil" or "metastatic niches") can be especially permissive for metastatic seeding and colonization by certain types of cancer cells, as a consequence of local properties that are either intrinsic to the normal tissue or induced at a distance by systemic actions of primary tumors. Cancer stem cells may be variably involved in some or all of the different stages of primary tumorigenesis and metastasis.

# Targeted therapies & Immunotherapies

Fig 2. Mechanisms of Akt's effect on glucose uptake and glycolysis

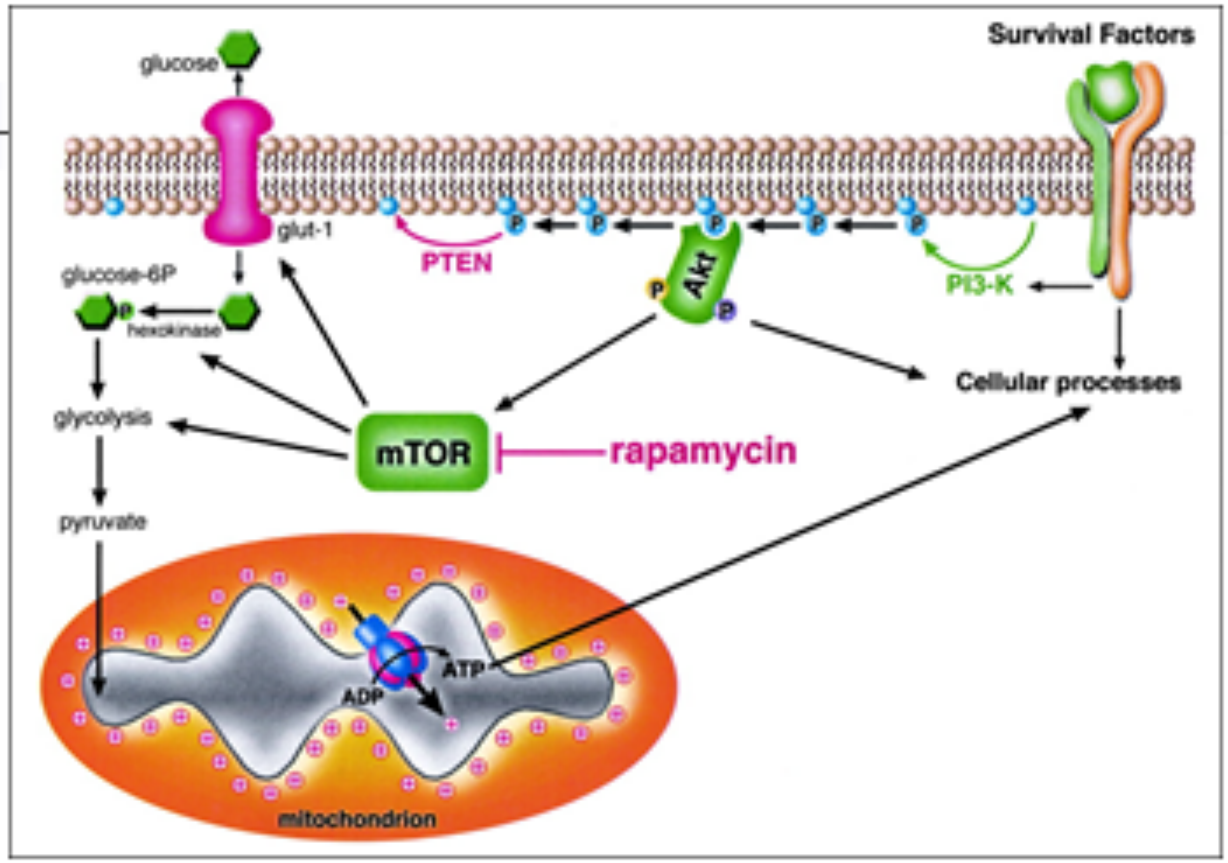


Thompson, J. E. et al. J Clin Oncol; 22:4217-4226 2004

VOLUME 25 · NUMBER 13 · MAY 1 2007

JOURNAL OF CLINICAL ONCOLOGY ORIGINAL REPORT

# Correlation of Computed Tomography and Positron Emission Tomography in Patients With Metastatic Gastrointestinal Stromal Tumor Treated at a Single Institution With Imatinib Mesylate: Proposal of New Computed Tomography Response Criteria

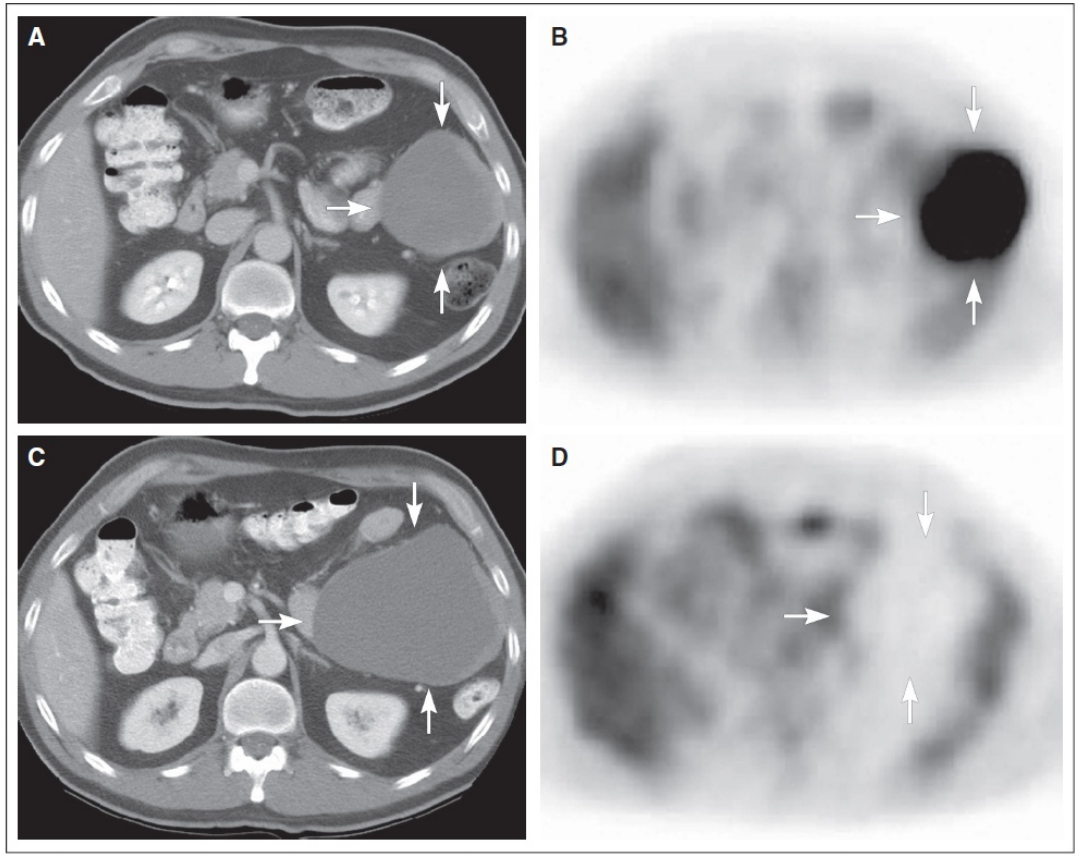


**Fig 5.** A 51-year-old male with primary gastrointestinal stromal tumors of colon and recurrent peritoneal metastases. Pretreatment computed tomography (CT) scan shows (A) a relatively low-density peritoneal mass (42 Hounsfield units [HU]) (→) corresponding to (B) a lesion with markedly increased glucose uptake (→) on positron emission tomography using [$^{18}$F]fluorodeoxyglucose (FDG-PET). At 2 months after treatment, (C) the mass (→) has become larger, however, the CT density has decreased (30 HU), (D) with no appreciable glucose uptake (→) on FDG-PET, corresponding to clinical improvement. (Reprinted with permission.[11])

**Table 3.** Modified CT Response Evaluation Criteria

| Response | Definition |
|---|---|
| CR | Disappearance of all lesions |
| | No new lesions |
| PR | A decrease in size* of ≥ 10% or a decrease in tumor density (HU) ≥ 15% on CT |
| | No new lesions |
| | No obvious progression of nonmeasurable disease |
| SD | Does not meet the criteria for CR, PR, or PD |
| | No symptomatic deterioration attributed to tumor progression |
| PD | An increase in tumor size of ≥ 10% and does not meet criteria of PR by tumor density (HU) on CT |
| | New lesions |
| | New intratumoral nodules or increase in the size of the existing intratumoral nodules |

Abbreviations: CR, complete response; PR, partial response; HU, Hounsfield unit; CT, computed tomography; SD, stable disease; PD, progression of disease; RECIST, Response Evaluation Criteria in Solid Tumors.
*The sum of longest diameters of target lesions as defined in RECIST.[10]

**Table 4.** Response Rates by RECIST, FDG-PET, and Modified CT Criteria (N = 40)

| Outcome | RECIST | FDG-PET | CT |
|---|---|---|---|
| Responders (n) | 17 | 33 | 32 |
| Nonresponders (n) | 23 | 7 | 8 |
| Response rate (%) | 43 | 83 | 80 |

Abbreviations: RECIST, Response Evaluation Criteria in Solid Tumors; FDG-PET, [$^{18}$F]fluorodeoxyglucose positron emission tomography; CT, computed tomography.

Eur J Nucl Med Mol Imaging (2016) 43:1792–1801
DOI 10.1007/s00259-016-3365-x

ORIGINAL ARTICLE

# Monitoring metabolic response using FDG PET-CT during targeted therapy for metastatic colorectal cancer

Erwin Woff[1] · Alain Hendlisz[2] · Camilo Garcia[1] · Amelie Deleporte[2] · Thierry Delaunoit[3] · Raphaël Maréchal[4] · Stéphane Holbrechts[5] · Marc Van den Eynde[6] · Gauthier Demolin[7] · Irina Vierasu[8] · Renaud Lhommel[9] · Namur Gauthier[10] · Thomas Guiot[1] · Lieveke Ameye[11] · Patrick Flamen[1]

An imaging biomarker for early non-response detection should have a high negative predictive value to avoid unjustified early discontinuation of an effective treatment. False-negative early responses should be avoided through the use of a low response cut-off, with a decrease of FDG uptake (expressed as $SUV_{max}$) of less than 15 % compared to baseline [15].

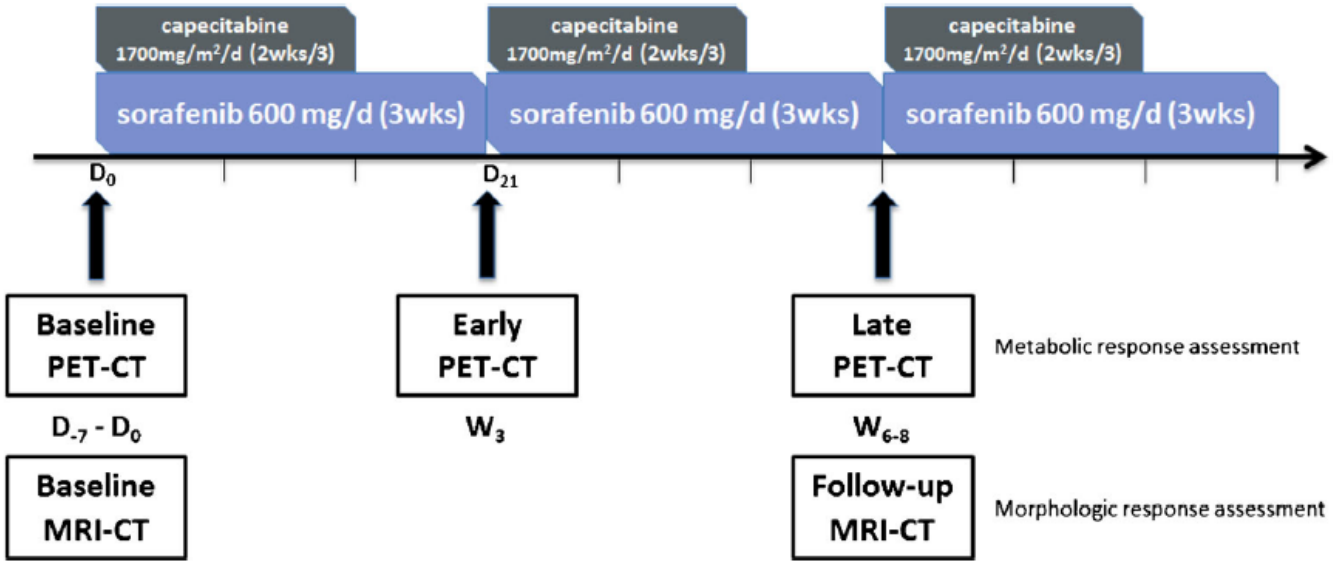

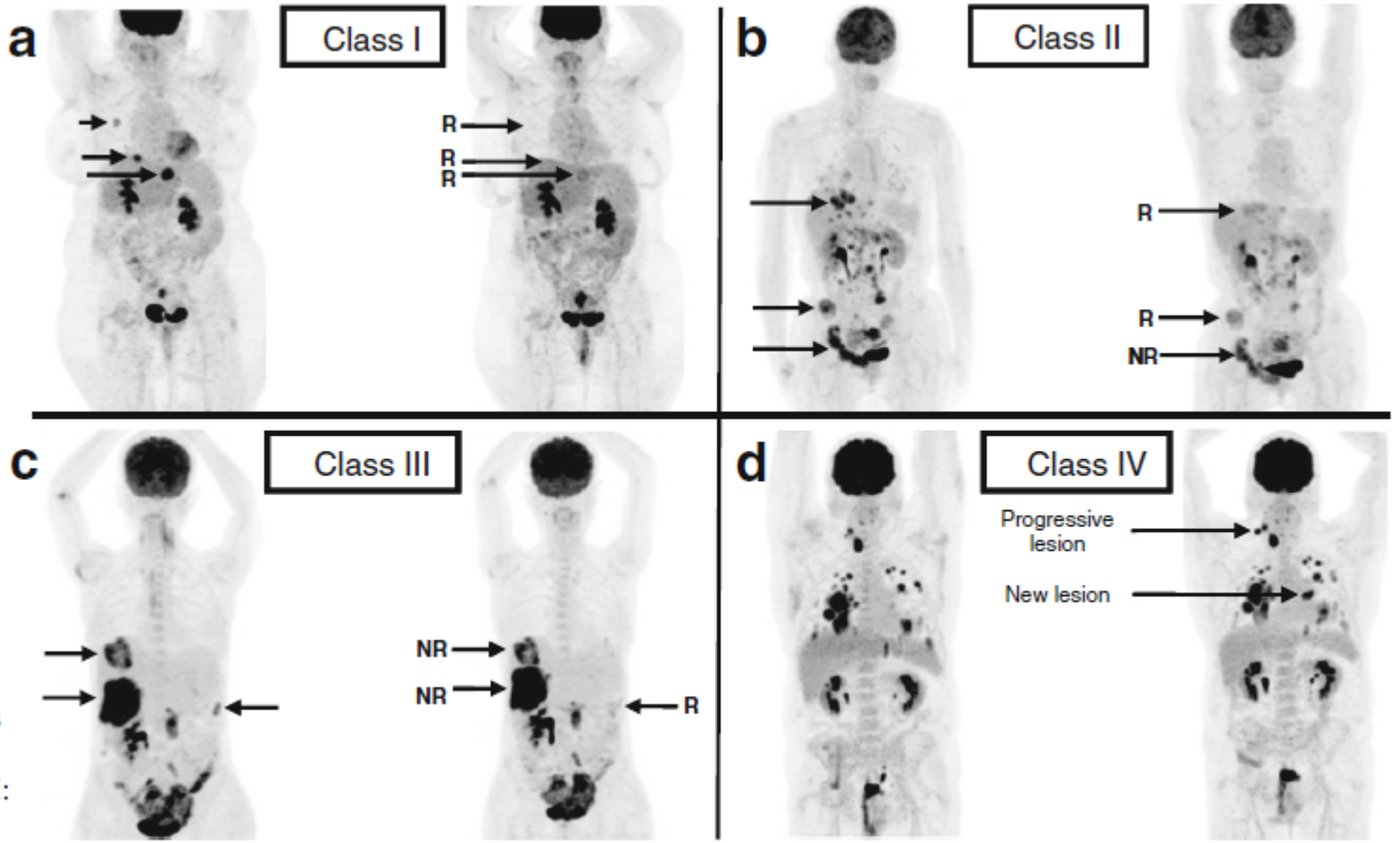


**Fig. 2** Representative examples of each metabolic dominance response classification. **a** Class I: absence of non-responding lesions **b** Class II: mixed response with a minor proportion of non-responding tumour load **c** Class III: mixed response with a major proportion of non-responding tumour load **d** Class IV: all lesions showed non-response, or the presence of at least one progressive lesion or the appearance of a new lesion

**Table 3** Agreement on lesion-based mR between early and late PET

| Metabolic response | | Late PET | | | | |
|---|---|---|---|---|---|---|
| | | mCR | mPR | mSD | mPD | Total |
| Early PET | mCR | 5 | 0 | 0 | 0 | 5 |
| | mPR | 10 | 55 | 13 | 0 | 78 |
| | mSD | 0 | 6 | 20 | 1 | 27 |
| | mPD | 0 | 0 | 4 | 10 | 14 |
| Total | | 15 | 61 | 37 | 11 | 124 |

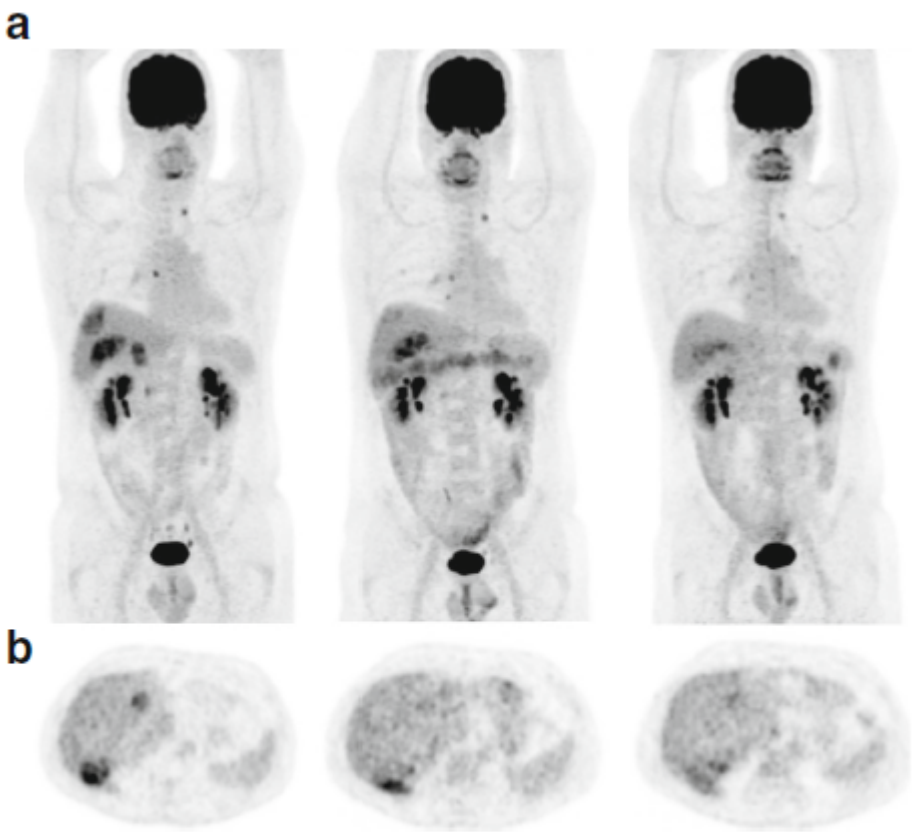


**Fig. 3** Illustration of the metabolic discordant response between early and late PET evaluations. **a** Patient-based discordant mR: baseline coronal maximum intensity projection (MIP) showing two highly metabolic right hepatic lesions (*left*), week 3 MIP mixed mR of hepatic target lesions (class II) (*middle*), and week 6 MIP homogenous mR of all hepatic target lesions (class I) (*right*). **b** Lesion-based discordant mR: baseline axial PET slice showing the two highly metabolic right hepatic lesions (*left*), week 3 PET mSD of the right posterior hepatic lesion and mCR of the hepatic dome lesion (*middle*), and week 6 PET mPR of the right posterior hepatic lesion (*right*)

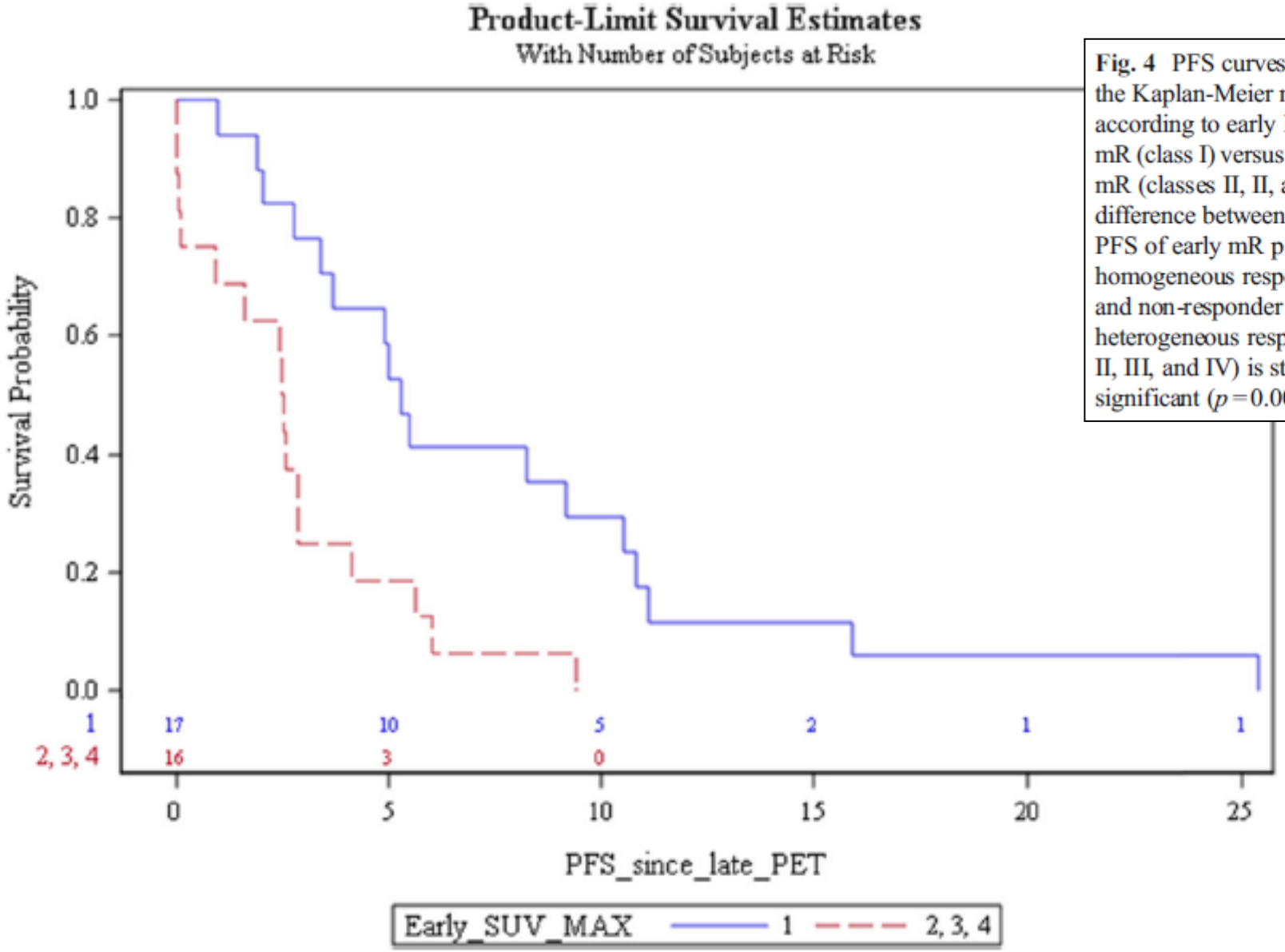


**Fig. 4** PFS curves estimated by the Kaplan-Meier method according to early homogeneous mR (class I) versus heterogeneous mR (classes II, II, and IV). The difference between the median PFS of early mR patients with a homogeneous response (class I) and non-responder patients with a heterogeneous response (classes II, III, and IV) is statistically significant ($p = 0.003$)

# The Predictive Value of Early In-Treatment $^{18}$F-FDG PET/CT Response to Chemotherapy in Combination with Bevacizumab in Advanced Nonsquamous Non–Small Cell Lung Cancer

Edwin A. Usmanij[1], Tinatin Natroshvili[1], Johanna N.H. Timmer-Bonte[2], Wim J.G. Oyen[1,3], Miep A. van der Drift[4], Johan Bussink[5], and Lioe-Fee de Geus-Oei[1,6]

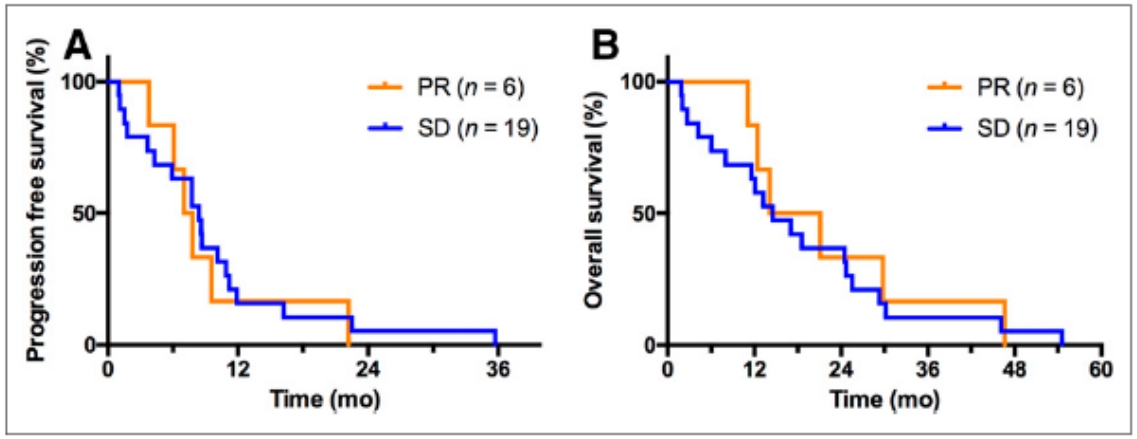


J Nucl Med 2017; 58:1243–1248

**FIGURE 2.** Kaplan–Meier analysis of PFS and OS stratified using RECIST. For stable disease (SD), median PFS was 8.4 and median OS was 14.5 mo. For partial response (PR), median PFS was 7.4 mo and median OS was 17.6 mo. Log-rank test, $P$ = not significant.

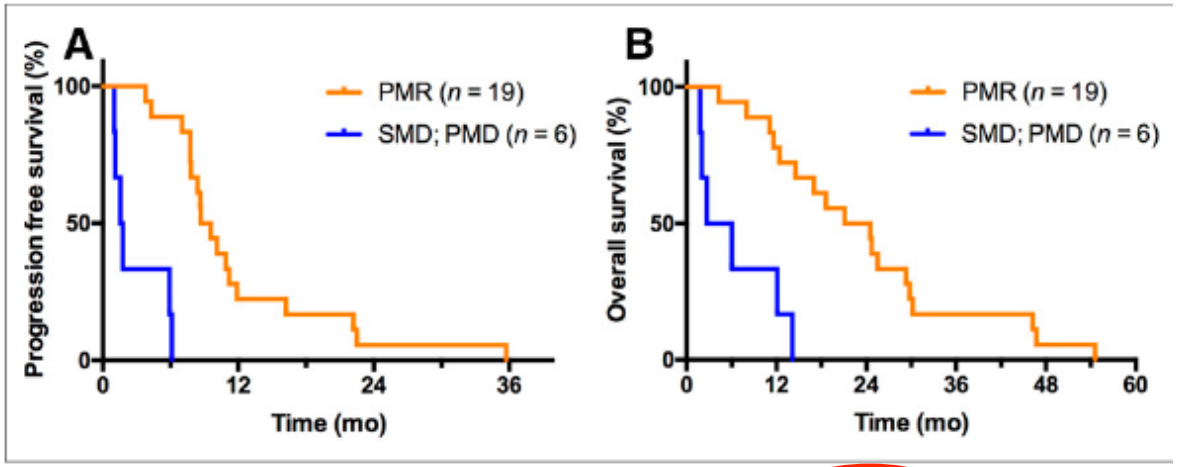


**FIGURE 3.** Kaplan–Meier analysis of PFS and OS stratified using PERCIST. For SMD and PMD median PFS was 1.7 mo and median OS was 4.4 mo. For PMR, median PFS was 9.1 mo and OS was 22.8 mo. Log-rank test, $P < 0.001$.

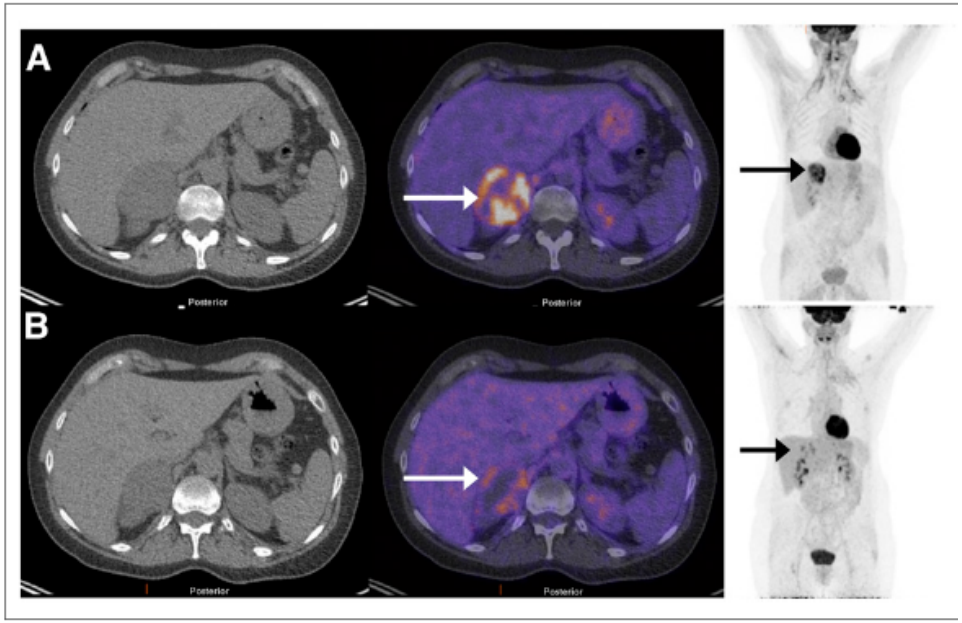


**FIGURE 4.** Baseline (A) and in-treatment (B) $^{18}$F-FDG PET/CT in a 51-y-old female patient wit NSCLC, stage IVB, with Pancoast tumor in left lung with metastasis in right adrenal gland (whit and black arrows). In-treatment $^{18}$F-FDG PET/CT showed apparent decrease in uptake classifie as PMR. Survival was 12.4 mo.

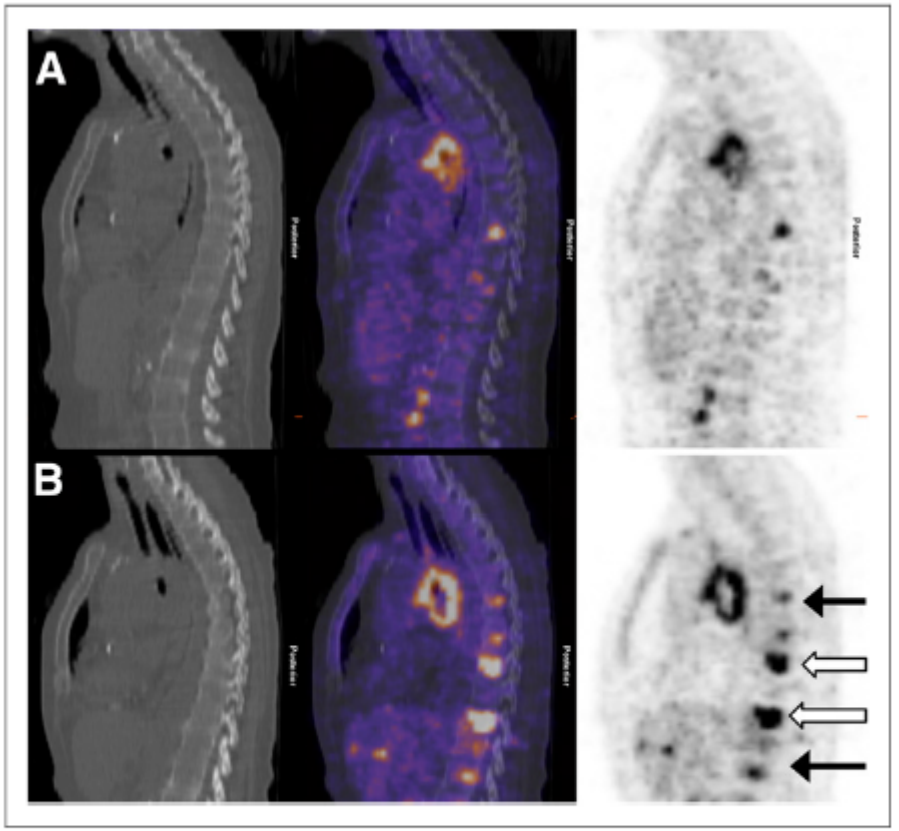


**FIGURE 5.** Baseline (A) and in-treatment (B) $^{18}$F-FDG PET/CT in a 67-y-old female patient with NSCLC, stage IVB, with tumor in left lower lobe with metastases in lymph nodes, lung, liver, and bones. In-treatment $^{18}$F-FDG PET/CT showed apparent increase in uptake (open arrows) and new $^{18}$F-FDG–avid bone lesions (black arrows), classified as PMD.

Comparison of In-Treatment Response Between PERCIST and RECIST

| | RECIST | | | |
|---|---|---|---|---|
| PERCIST | Complete response ($n$ = 0) | Partial response ($n$ = 6) | Stable disease ($n$ = 19) | Progressive disease ($n$ = 0) |
| CMR ($n$ = 0) | 0 | 0 | 0 | 0 |
| PMR ($n$ = 19) | 0 | 5 | 14 | 0 |
| SMD ($n$ = 4) | 0 | 1 | 3 | 0 |
| PMD ($n$ = 2) | 0 | 0 | 2 | 0 |

# The Immunotherapy Landscape in Oncology

Immunotherapy continues to be a growing category in oncology treatment, and company- and cooperative group-sponsored trials are being conducted in all major tumor types.

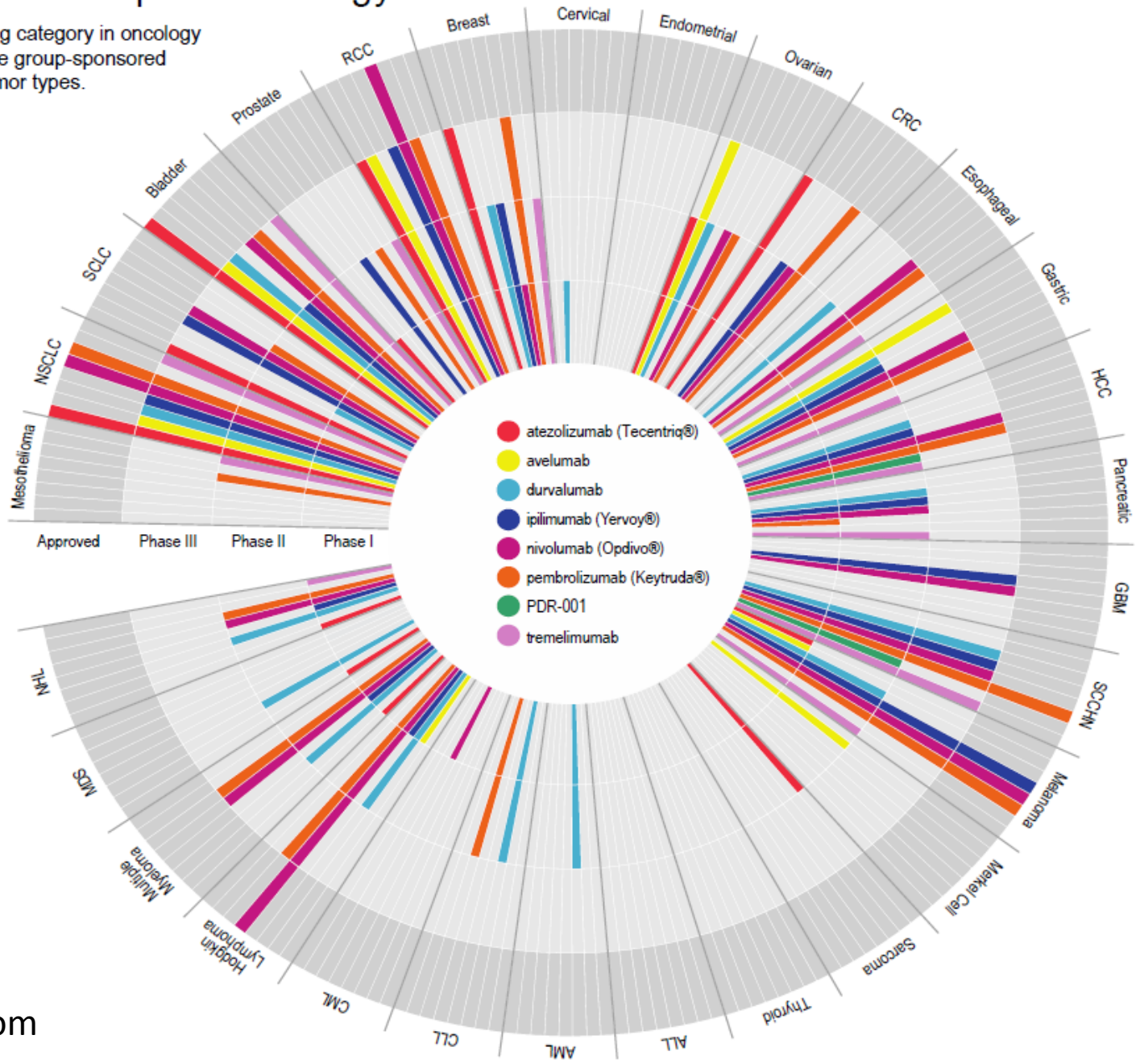


www.kantarhealth.com

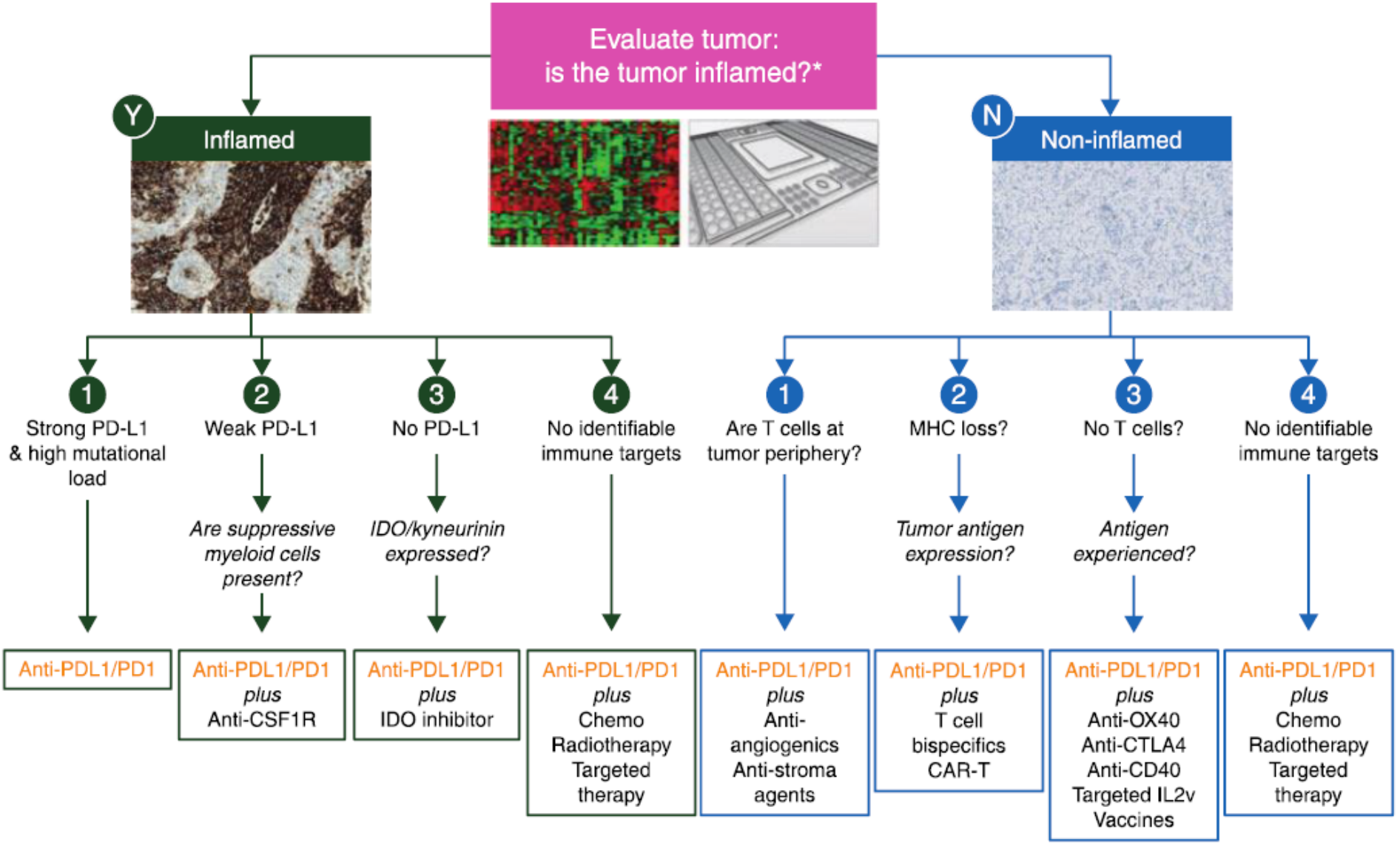


« Programmed-Death (Ligand ) 1 »

## Special features of the response to immunotherapies

- Delayed or late response
- Frequent initial "pseudo-progression"
- Sustainable stabilizations = success
- Dissociated clinical responses ≠ failure!
- In case of progression, stop treatment not always indicated: there may be a response afterwards ... reassessment at 4 weeks
- Improvement of the overall survival without improvement of the PFS!

# Guidelines for the Evaluation of Immune Therapy Activity in Solid Tumors: Immune-Related Response Criteria

Clin Cancer Res 2009;15(23) December 1, 2009

Jedd D. Wolchok,[1] Axel Hoos,[2] Steven O'Day,[3] Jeffrey S. Weber,[4] Omid Hamid,[3] Celeste Lebbé,[5] Michele Maio,[6] Michael Binder,[7] Oliver Bohnsack,[8] Geoffrey Nichol,[9] Rachel Humphrey,[2] and F. Stephen Hodi[10]

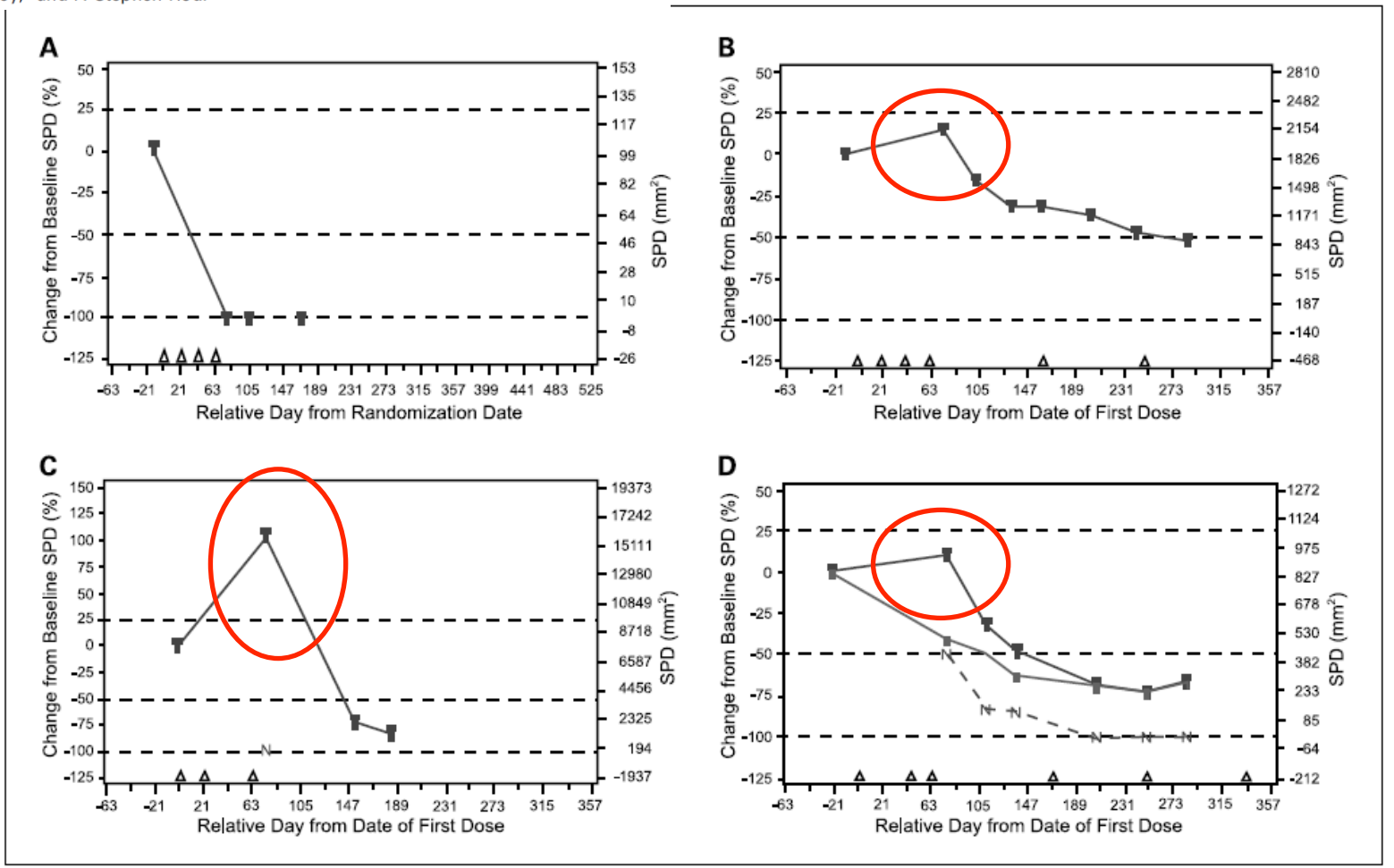


**Fig. 1.** Patterns of response to ipilimumab observed in advanced melanoma. Shown are the four response patterns observed in advanced melanoma patients treated with ipilimumab at 10 mg/kg in the CA184-008 and CA184-022 studies. *A*, response in baseline lesions; *B*, "stable disease" with slow, steady decline in total tumor volume; *C*, response after initial increase in total tumor volume; *D*, reduction in total tumor burden after the appearance of new lesions. SPD, sum of the product of perpendicular diameters. N, tumor burden of new lesions (*C* and *D*). *D*, top line, total tumor burden; middle line, tumor burden of baseline lesions; bottom line, tumor burden of new lesions. Triangles, ipilimumab dosing time points; dashed lines, thresholds for response or PD/irPD.

Eur J Nucl Med Mol Imaging
DOI 10.1007/s00259-017-3806-1

ORIGINAL ARTICLE

Nivolumab, an immune checkpoint inhibitor developed as an anti-programmed death-1 (PD-1) antibody, was recently approved in patients with previously treated NSCLC [3, 4]. Two

# Metabolic activity by $^{18}$F–FDG-PET/CT is predictive of early response after nivolumab in previously treated NSCLC

Kyoichi Kaira[1] · Tetsuya Higuchi[2] · Ichiro Naruse[3] · Yukiko Arisaka[2] · Azusa Tokue[2] · Bolag Altan[1] · Satoshi Suda[4] · Akira Mogi[5] · Kimihiro Shimizu[5] · Noriaki Sunaga[6] · Takeshi Hisada[7] · Shigehisa Kitano[8] · Hideru Obinata[9] · Takehiko Yokobori[10] · Keita Mori[11] · Masahiko Nishiyama[12] · Yoshihito Tsushima[2,13] · Takayuki Asao[9]

Published online: 21 August 2017

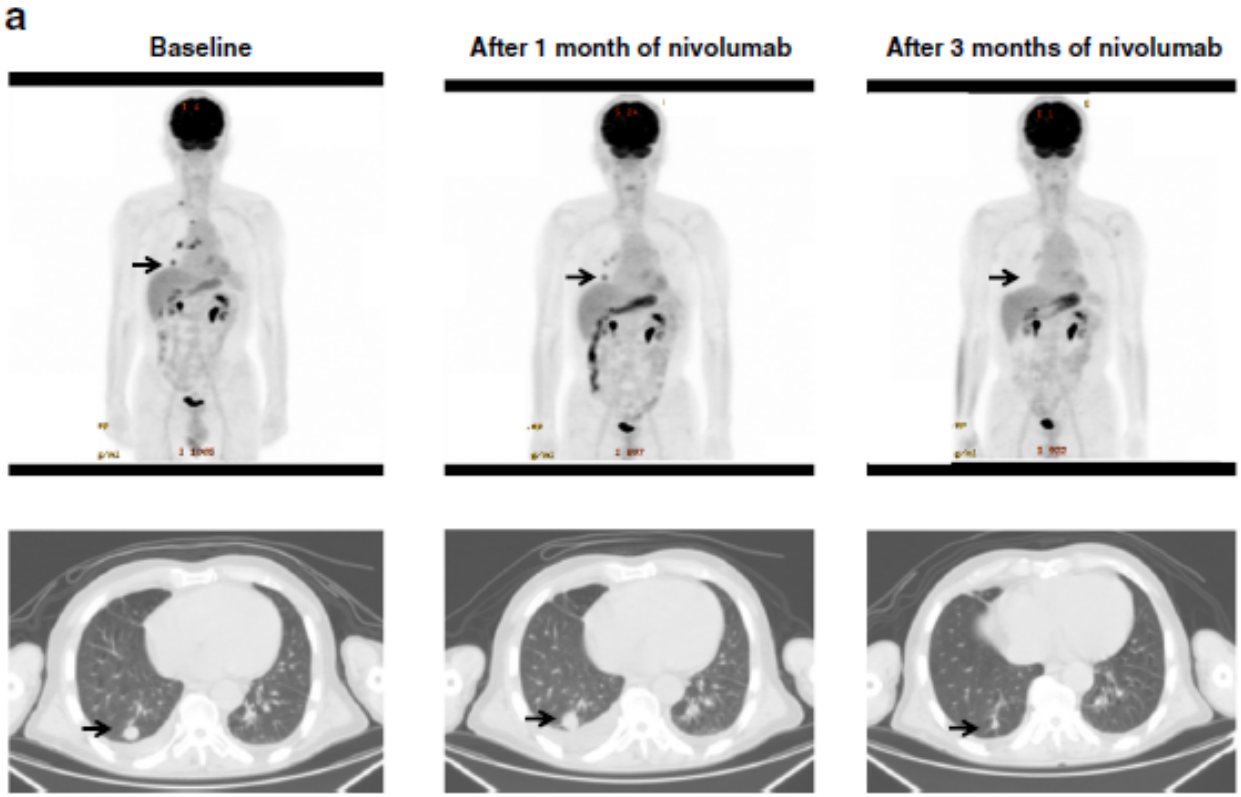

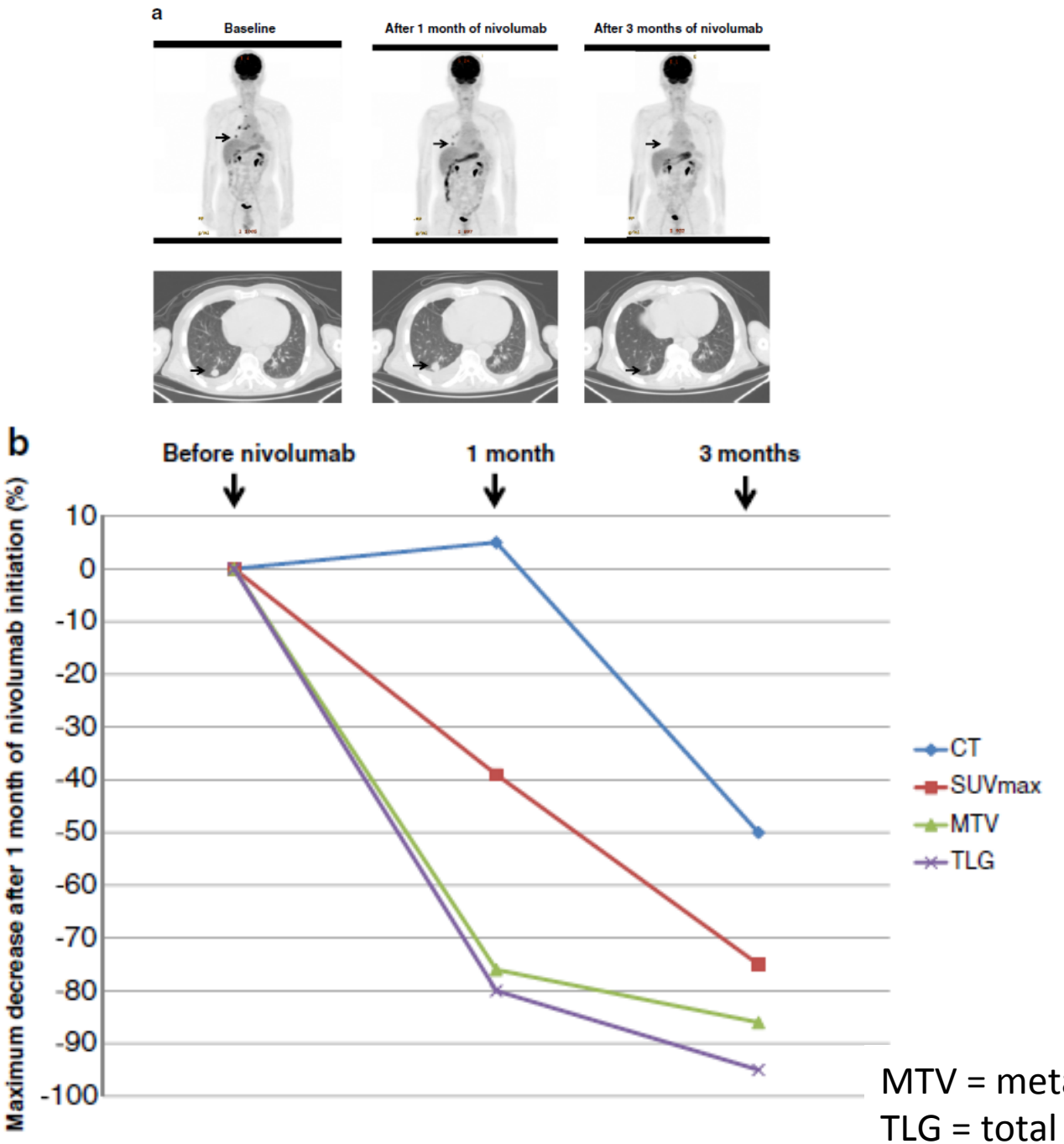


MTV = metabolic tumour volume
TLG = total lesion glycolysis

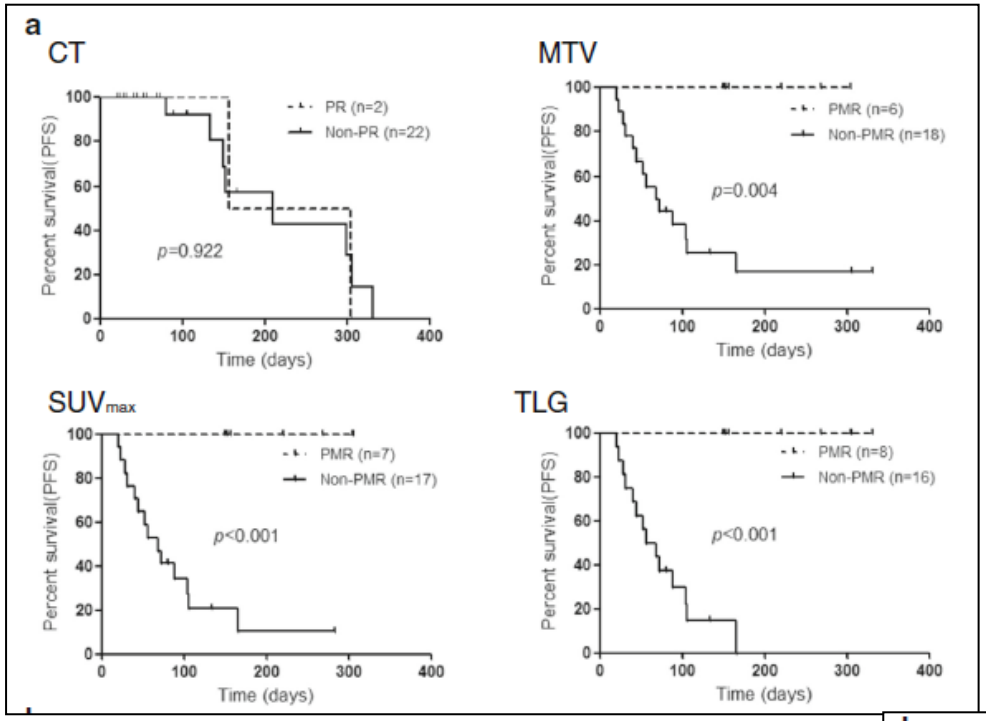
a
CT
PR (n=2)
Non-PR (n=22)
p=0.922
Percent survival(PFS)
Time (days)
MTV
PMR (n=6)
Non-PMR (n=18)
p=0.004
Percent survival(PFS)
Time (days)
SUVmax
PMR (n=7)
Non-PMR (n=17)
p<0.001
Percent survival(PFS)
Time (days)
TLG
PMR (n=8)
Non-PMR (n=16)
p<0.001
Percent survival(PFS)
Time (days)

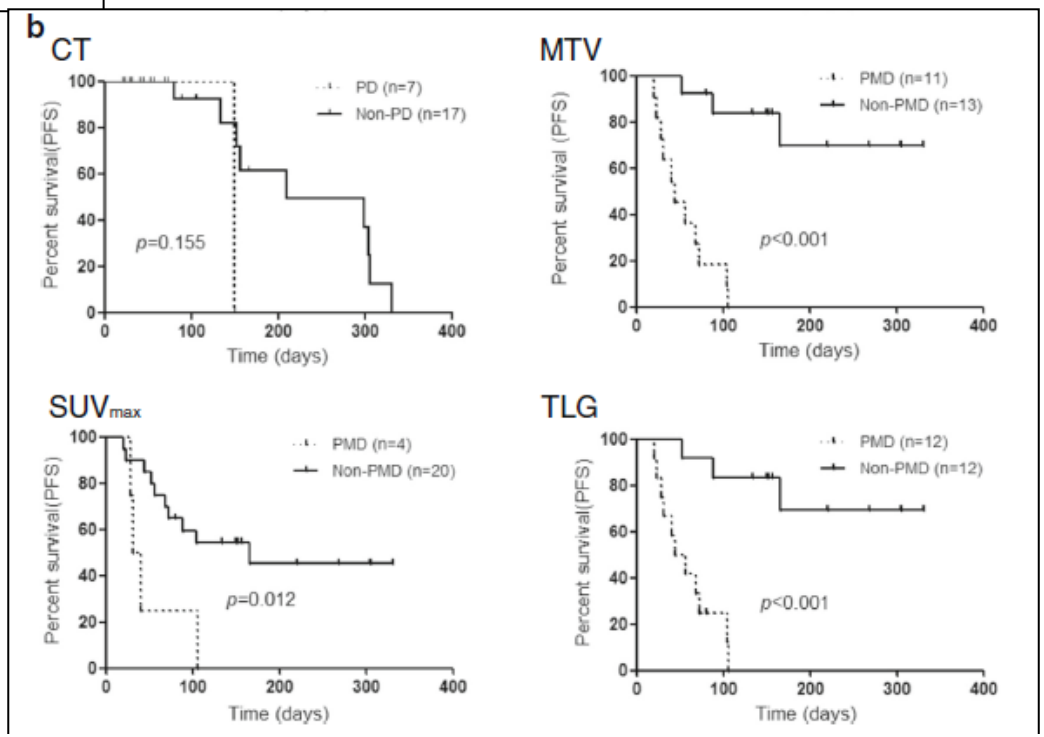
b
CT
PD (n=7)
Non-PD (n=17)
p=0.155
Percent survival(PFS)
Time (days)
MTV
PMD (n=11)
Non-PMD (n=13)
p<0.001
Percent survival (PFS)
Time (days)
SUVmax
PMD (n=4)
Non-PMD (n=20)
p=0.012
Percent survival(PFS)
Time (days)
TLG
PMD (n=12)
Non-PMD (n=12)
p<0.001
Percent survival(PFS)
Time (days)

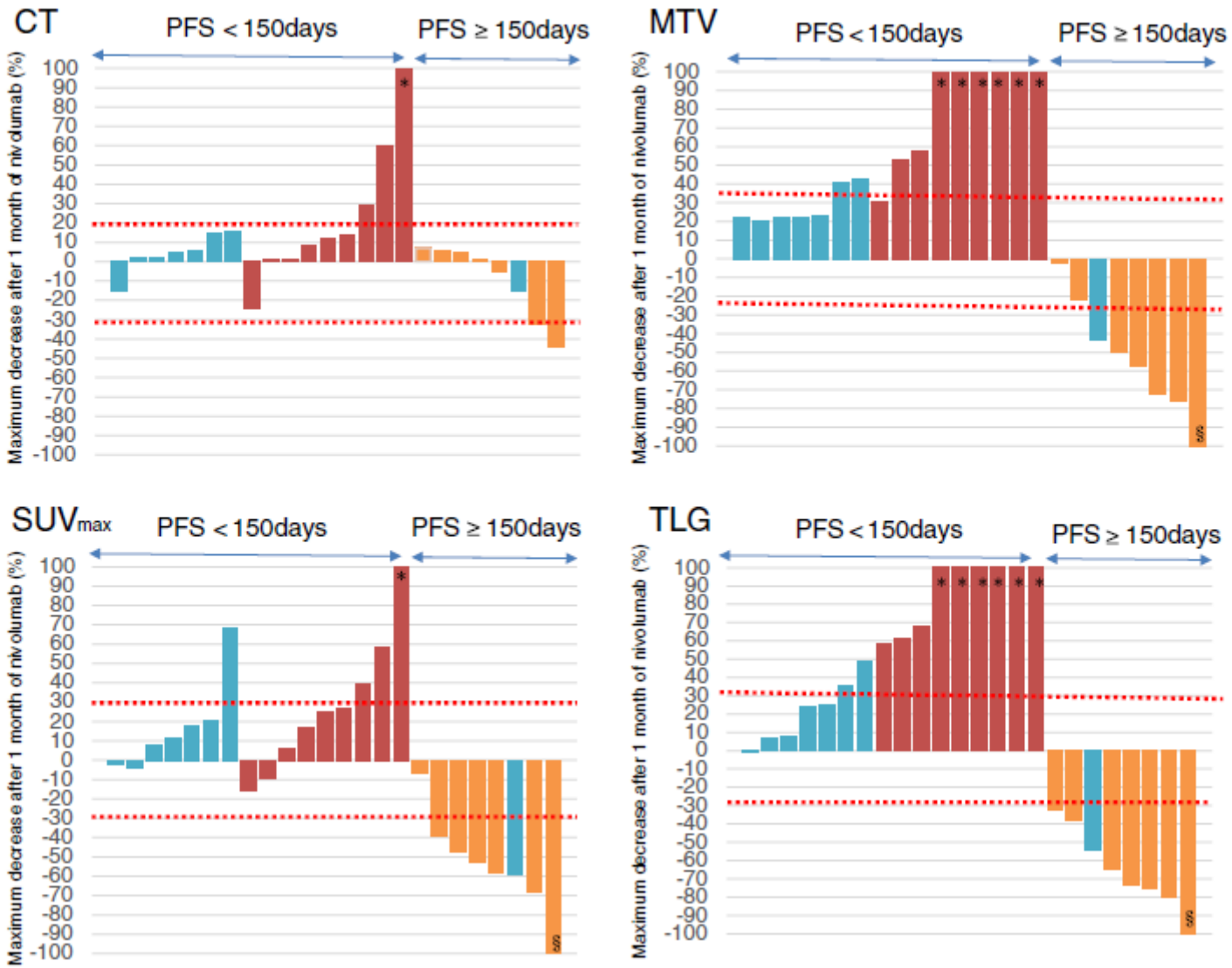
CT
PFS < 150days
PFS ≥ 150days
Maximum decrease after 1 month of nivolumab (%)
MTV
PFS < 150days
PFS ≥ 150days
Maximum decrease after 1 month of nivolumab (%)
SUVmax
PFS < 150days
PFS ≥ 150days
Maximum decrease after 1 month of nivolumab (%)
TLG
PFS < 150days
PFS ≥ 150days
Maximum decrease after 1 month of nivolumab (%)

Eur J Nucl Med Mol Imaging
DOI 10.1007/s00259-017-3813-2

SHORT COMMUNICATION

# 18F-FDG-PET detects complete response to PD1-therapy in melanoma patients two weeks after therapy start

Published online: 22 August 2017

Ferdinand Seith[1] · Andrea Forschner[2] · Holger Schmidt[1] · Christina Pfannenberg[1] · Brigitte Gückel[1] · Konstantin Nikolaou[1,3] · Christian la Fougère[3,4] · Claus Garbe[2] · Nina Schwenzer[1]

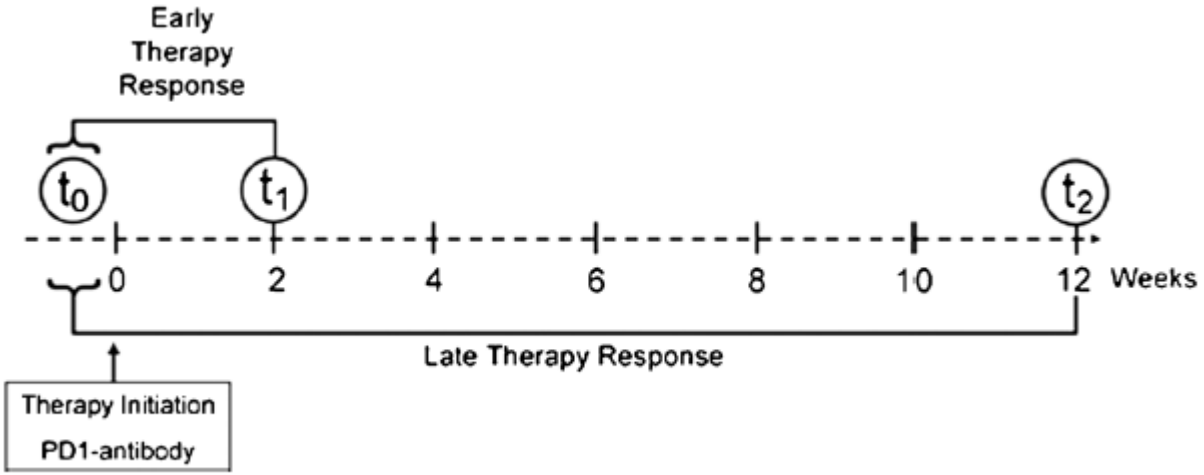


In conclusion, the preliminary results of our study indicate that whole-body 18F-FDG-PET might be able to reliably identify complete responders to PD1-therapy as early as two weeks after therapy initiation in stage IV melanoma patients. This might help to shorten therapy regimes and avoid unnecessary side effects in the future.

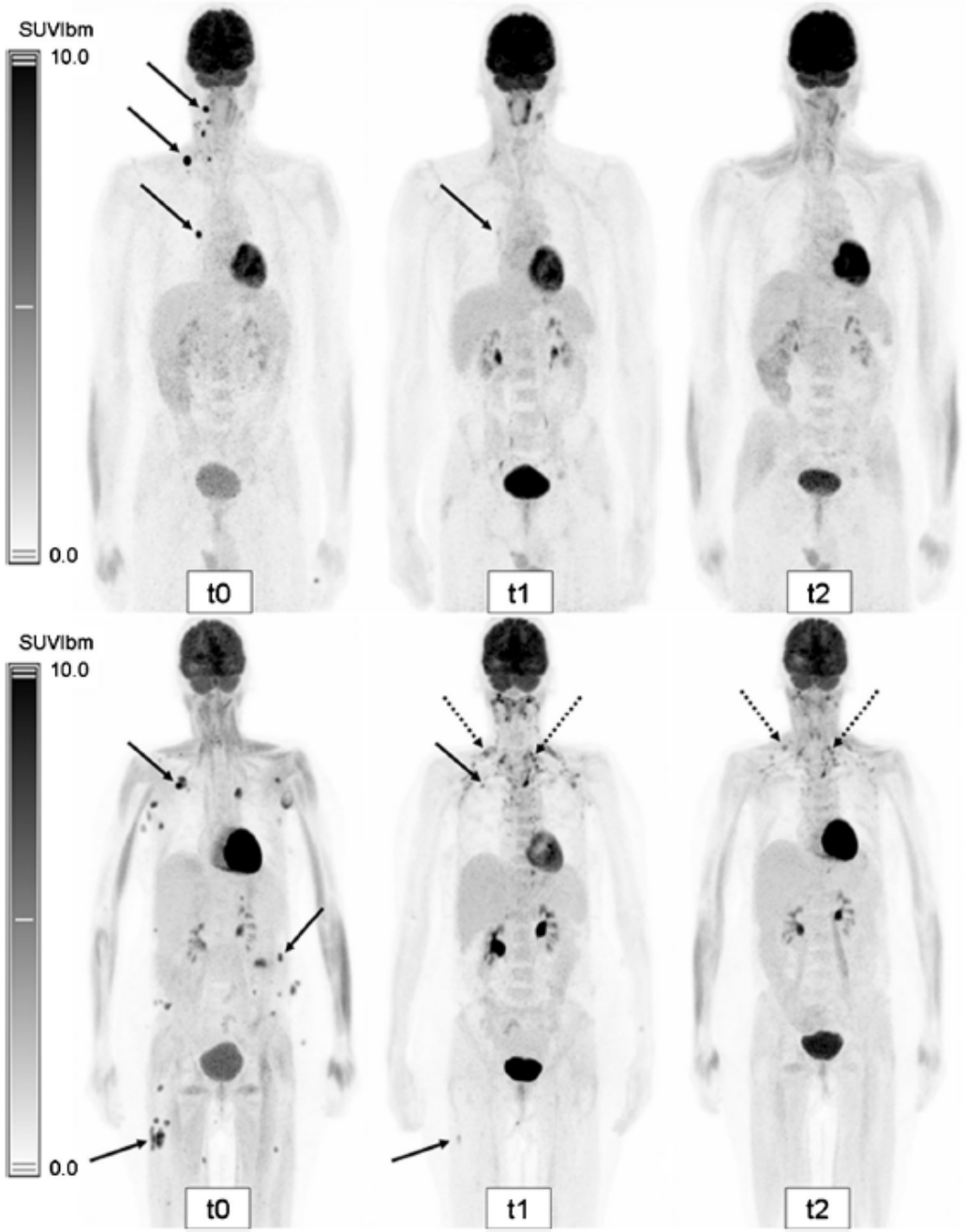


**Fig. 2** Two examples (Patients no. 4 and 10) of CMR after 12 weeks of PD1-therapy. Upper row: The patient suffered from metastases in the soft tissue, the lymph nodes and the lung at the baseline scan $t_0$ (black arrows). At $t_1$, only remnants of metastases are visible in the lung. Lower row: The patient suffered from multiple soft tissue metastases (black arrows); at $t_1$, only remnants of metastases are visible, e.g., at the thigh and the pectoral region; increased metabolic activity of brown adipose tissue at $t_1$ and $t_2$ (dotted arrows) should not be mistaken for metastases

VOLUME 34 · NUMBER 13 · MAY 1, 2016

JOURNAL OF CLINICAL ONCOLOGY

ORIGINAL REPORT

# Evaluation of Immune-Related Response Criteria and RECIST v1.1 in Patients With Advanced Melanoma Treated With Pembrolizumab

*F. Stephen Hodi, Wen-Jen Hwu, Richard Kefford, Jeffrey S. Weber, Adil Daud, Omid Hamid, Amita Patnaik, Antoni Ribas, Caroline Robert, Tara C. Gangadhar, Anthony M. Joshua, Peter Hersey, Roxana Dronca, Richard Joseph, Darcy Hille, Dahai Xue, Xiaoyun Nicole Li, S. Peter Kang, Scot Ebbinghaus, Andrea Perrone, and Jedd D. Wolchok*

**Table 1.** Comparison of Key Differences in RECIST v1.1 and irRC

| Category | RECIST v1.1 | irRC |
|---|---|---|
| Measurement of tumor burden | Unidimensional | Bidimensional |
| Target lesions | Maximum, 5* | Maximum, 15 index lesions |
| New lesion | Results in progressive disease at first appearance | Up to 10 new visceral lesions and 5 cutaneous lesions may be added to the sum of the products of the two largest perpendicular diameters of all index lesions at any time point |
| Complete response | Disappearance of all target and nontarget lesions<br>Nodes must regress to < 10 mm short axis<br>No new lesions<br>Confirmation required | |
| Partial response | ≥ 30% decrease in tumor burden compared with baseline<br>Confirmation required | ≥ 50% decrease in tumor burden compared with baseline†<br>Confirmation required |
| Progressive disease | ≥ 20% + 5-mm absolute increase in tumor burden compared with nadir<br>Appearance of new lesions or progression of nontarget lesions | ≥ 25% increase in tumor burden compared with baseline, nadir, or reset baseline†<br>New lesions added to tumor burden<br>Confirmation required |
| Stable disease | Neither partial response nor progressive disease | |

Abbreviations: irRC, immune-related response criteria; RECIST v1.1, Response Evaluation Criteria in Solid Tumors, version 1.1.
*For the present analyses, the maximum number of target lesions was 10.
†If an increase in tumor burden is observed at the first scheduled assessment, the baseline is reset to the value observed at the first assessment.

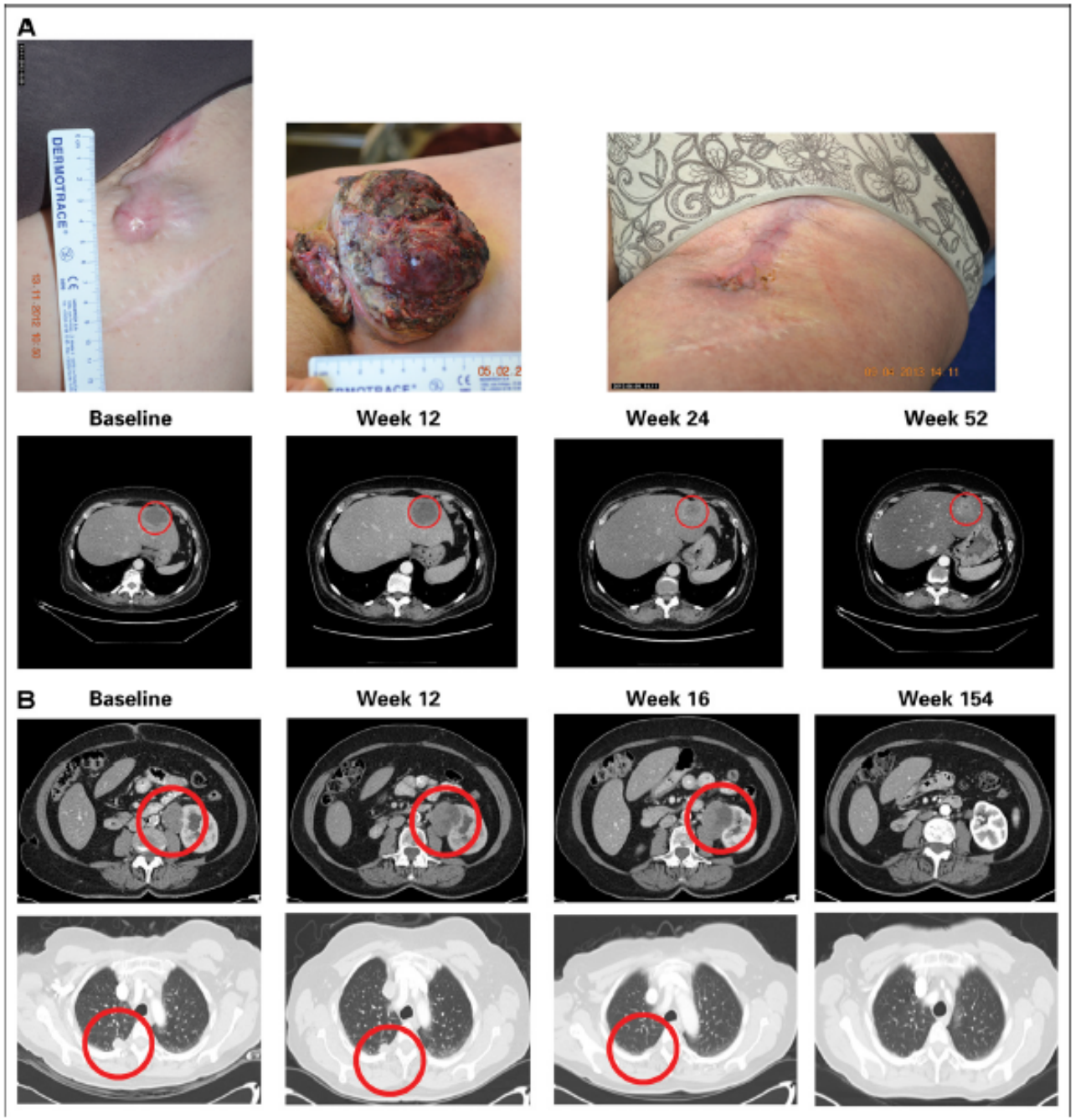


*J Clin Oncol 34:1510-1517.*

Case of « pseudo-progression »

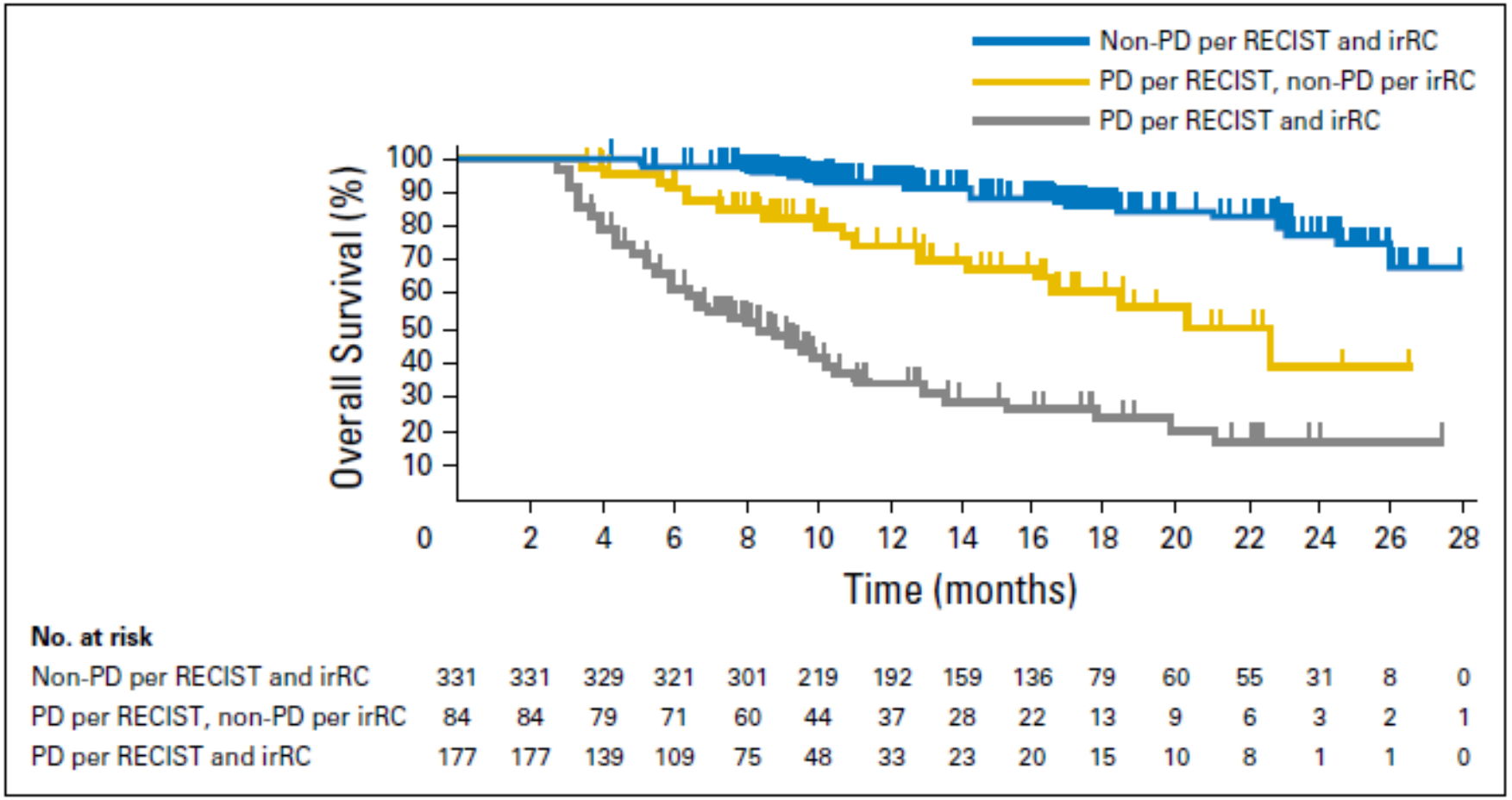


**No. at risk**

| | | | | | | | | | | | | | | | |
|---|---|---|---|---|---|---|---|---|---|---|---|---|---|---|---|
| Non-PD per RECIST and irRC | 331 | 331 | 329 | 321 | 301 | 219 | 192 | 159 | 136 | 79 | 60 | 55 | 31 | 8 | 0 |
| PD per RECIST, non-PD per irRC | 84 | 84 | 79 | 71 | 60 | 44 | 37 | 28 | 22 | 13 | 9 | 6 | 3 | 2 | 1 |
| PD per RECIST and irRC | 177 | 177 | 139 | 109 | 75 | 48 | 33 | 23 | 20 | 15 | 10 | 8 | 1 | 1 | 0 |

# Prediction of Response to Immune Checkpoint Inhibitor Therapy Using Early-Time-Point $^{18}$F-FDG PET/CT Imaging in Patients with Advanced Melanoma

J Nucl Med 2017; 58:1421–1428

Steve Y. Cho*[1,2], Evan J. Lipson*[1], Hyung-Jun Im*[2,3], Steven P. Rowe[1], Esther Mena Gonzalez[1], Amanda Blackford[1], Alin Chirindel[1], Drew M. Pardoll[1], Suzanne L. Topalian[1], and Richard L. Wahl[1,4]

Imm
ipilimu
(e.g., a
objecti
and oth
nivolur
melano
that dif
therapi
thereof
tiation

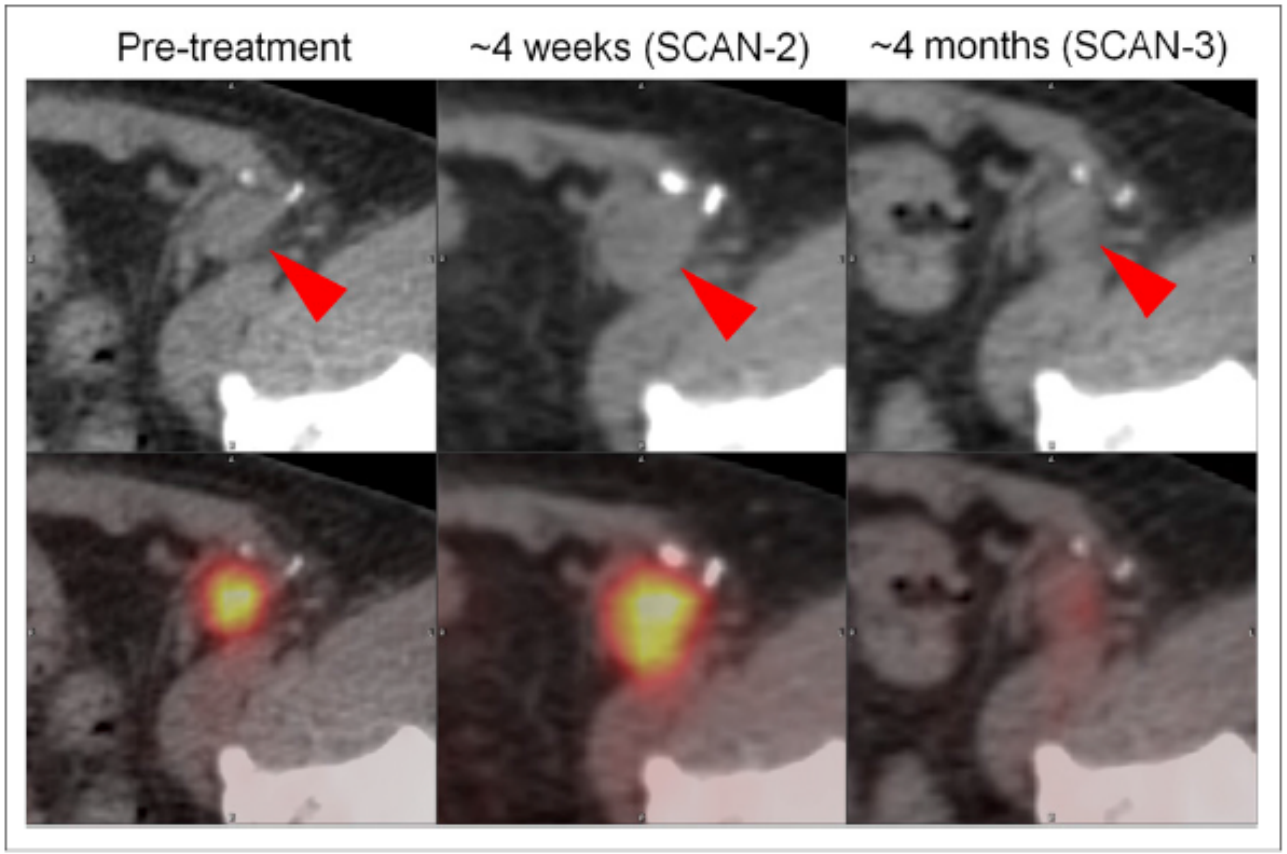


**FIGURE 3.** PET/CT images demonstrating representative changes in melanoma inguinal lymph node metastasis (red arrowheads) at 4 wk and 4 mo after initiation of ipilimumab. At about 4 wk

**TABLE 1**
Summary of Treatment Response Criteria

| Response | CT-based criteria | | PET-based criteria | | |
|---|---|---|---|---|---|
| | RECIST 1.1 | irRC | | PERCIST 1.0 | EORTC |
| Complete response | Disappearance of all TLs and NLs; all LNs < 10 mm short axis | Resolution of all lesions (whether measurable or not) and no new lesions | Complete metabolic response | Complete resolution of $^{18}$F-FDG uptake within measurable TL and disappearance of all other lesions to BBP levels | Complete resolution of $^{18}$F-FDG uptake within TV so that it is indistinguishable from surrounding NT |
| Partial response | ≥30% decrease in SoDs of TLs; NLs may persist but not unequivocally progress | Decrease in TB ≥ 50%, measured as SoPs of 2 largest perpendicular diameters of all ILs, relative to BL | Partial metabolic response | >30% RD and >0.8 AD in $SUL_{peak}$ of HL | Reduction of 15%–25% in tumor SUV after 1 CoT and >25% after more than 1 CoT |
| Stable disease | Neither sufficient TR nor TG to qualify for PR or PD | Not meeting criteria for irCR or irPR, in absence of irPD | Stable metabolic disease | Not meeting criteria for CMR, PMR, or PMD | Increase in tumor SUV of <25% or decrease of <15% and no visible increase in extent of $^{18}$F-FDG TU (20% in LD) |
| Progressive disease | ≥20% increase in sum of diameters of TLs or unequivocal progression of NL or appearance of new lesion | Increase in TB ≥ 25% relative to nadir, measured as SoPs of 2 largest perpendicular diameters of all ILs | Progressive metabolic disease | >30% RI and >0.8 AI in $SUL_{peak}$ of HL or unequivocal progression of $^{18}$F-FDG–avid NL or appearance of new $^{18}$F-FDG–avid lesion | Increase from BL in tumor SUV of >25% within tumor region, visible increase in extent of $^{18}$F-FDG TU (20% in LD), or appearance of new $^{18}$F-FDG uptake in MLs |

TL = target lesion; NL = nontarget lesion; LN = lymph node; BBP = background blood-pool; TV = tumor volume; NT = normal tissue; SoDs = sum of diameters; TB = tumor burden; SoPs = sum of the products; IL = index lesion; BL = baseline; RD = relative decrease; AD = absolute decrease; $SUL_{peak}$ = average SUV corrected by lean body mass within a 1-$cm^3$ spheric volume of interest; HL = hottest lesion; CoT = cycle of therapy; TR = tumor regression; TG = tumor growth; PR = partial response; PD = progressive disease; irCR = immune-related complete response; irPR = immune-related partial response; irPD = immune-related progressive disease; CMR = complete metabolic response; PMR = partial metabolic response; PMD = progressive metabolic disease; TU = tumor uptake; LD = longest dimension; RI = relative increase; AI = absolute increase; ML = metastatic lesion; SUV = for EORTC we used $SUV_{max}$ (maximum voxel value of SUV).

Immune checkpoint inhibitors

**TABLE 4**

Performance Characteristics of 5 Methods of Early Tumor Response Evaluation in Predicting Response (RECIST 1.1) to ICI Therapy at 4 Months

| Method no. | Tumor response evaluation method description | SCAN-1 to SCAN-2 optimal percentage change cutoff | Sensitivity (%) | Specificity (%) | PPV (%) | NPV (%) | Accuracy (%) |
|---|---|---|---|---|---|---|---|
| 1 | Change in sum of RECIST 1.1–based target lesion diameters | ≤0 | 80.0 (28.8–96.7) | 86.7 (59.5–98.0) | 66.7 (22.7–94.7) | 92.9 (66.1–98.8) | 85.0 |
| 2 | Change in sum of the products of the 2 largest perpendicular diameters of irRC-based index lesions | ≤ −14.7 | 60.0 (15.4–93.5) | 93.3 (68.0–98.9) | 75.0 (20.3–95.9) | 87.5 (61.6–98.1) | 85.0 |
| 3 | Change in SULpeak of the hottest lesion | >15.5 | 80.0 (28.8–96.7) | 73.3 (44.9–92.0) | 50.0 (16.0–84.0) | 91.7 (61.5–98.6) | 75.0 |
| 4 | Change in sum of $SUV_{max}$ of all $^{18}$F-FDG–avid metastatic lesions | >14.7 | 80.0 (28.8–96.7) | 66.7 (38.4–88.1) | 44.4 (14.0–78.6) | 90.9 (58.7–98.5) | 70.0 |
| | Methods 1 and 3, above, combined (PECRIT) | | 100.0 (48.0–100) | 93.3 (68.0–98.9) | 83.3 (36.1–97.2) | 100.0 (76.7–100.0) | 95.0 |

PPV = positive predictive value; NPV = negative predictive value; method 1 = change in sum of target lesion diameters, selected based on RECIST 1.1; method 2 = change in sum of the products of the 2 largest perpendicular diameters of index lesions, selected based on irRC criteria; method 3 = change in peak SUV, normalized by lean body mass, of the hottest lesion ($SUL_{peak}$) seen on PET scan (PERCIST 1.0); method 4 = change in the $SUV_{max}$ of all $^{18}$F-FDG–avid metastatic lesions; PECRIT = **PE**T/CT **C**riteria for early prediction of **R**esponse to **I**mmune checkpoint inhibitor **T**herapy.

Changes in tumor burden seen on PET/CT scans from baseline (SCAN-1) to 3–4 wk (SCAN-2) were calculated using 4 methods, each based on standard response criteria. Optimal cutoff percentage changes to predict response to ICI therapy based on RECIST 1.1 at 4 mo were determined from ROC analysis. Data in parentheses are 95% confidence intervals.

# Nuclear Imaging Probes: from Bench to Bedside

Clin Cancer Res 2007;13(12) June 15, 2007

Hans-Jürgen Wester

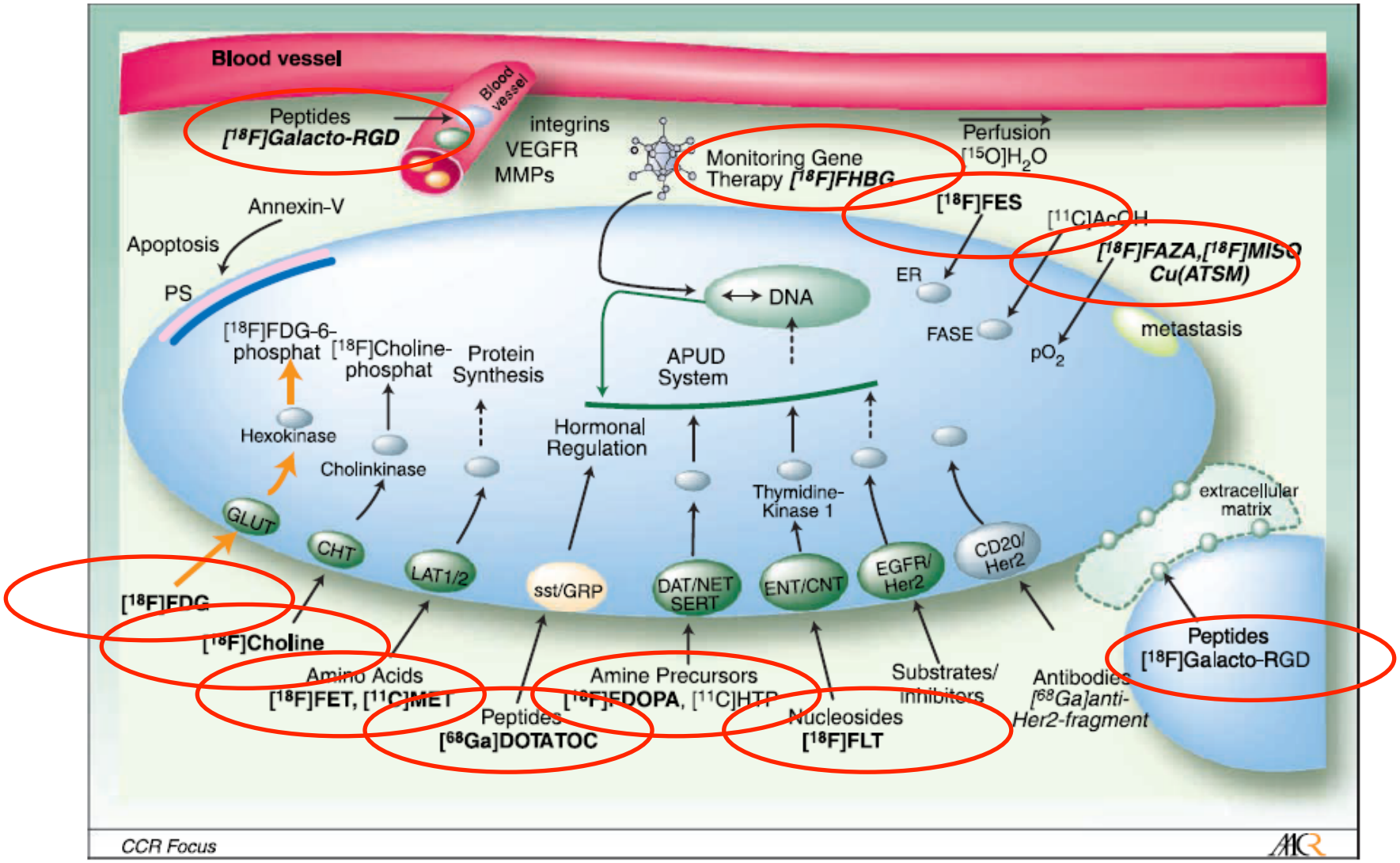


**Fig. 2.** Selected targets and corresponding nuclear imaging probes already established for nuclear molecular imaging in the clinic (*bold*) or currently under assessment in clinical studies (*italic*).

# Radiolabeled Choline

- **Choline = cell membrane turn-over marker**
  - **cell uptake : quick, specific, energy-dependant (mechanisms still to be depicted)**
  - **phosphorylation by choline kinase**
  - **phosphorylcholine ⇨ phosphatidylcholine**
    - **signal transduction**
    - **apoptosis…**

- **turn-over increased in tumour cells**

- **proliferation marker / membrane turnover = néoplastic celles**

- **≠ pick of choline en RMNs ++++++**

  (Rommel et al *Nucl Med Biol* 2010, Yagamushi et al *Eur J Nucl Med Biol Imag* 2005, Rommel et al *Mol Imaging Biol* 2010)

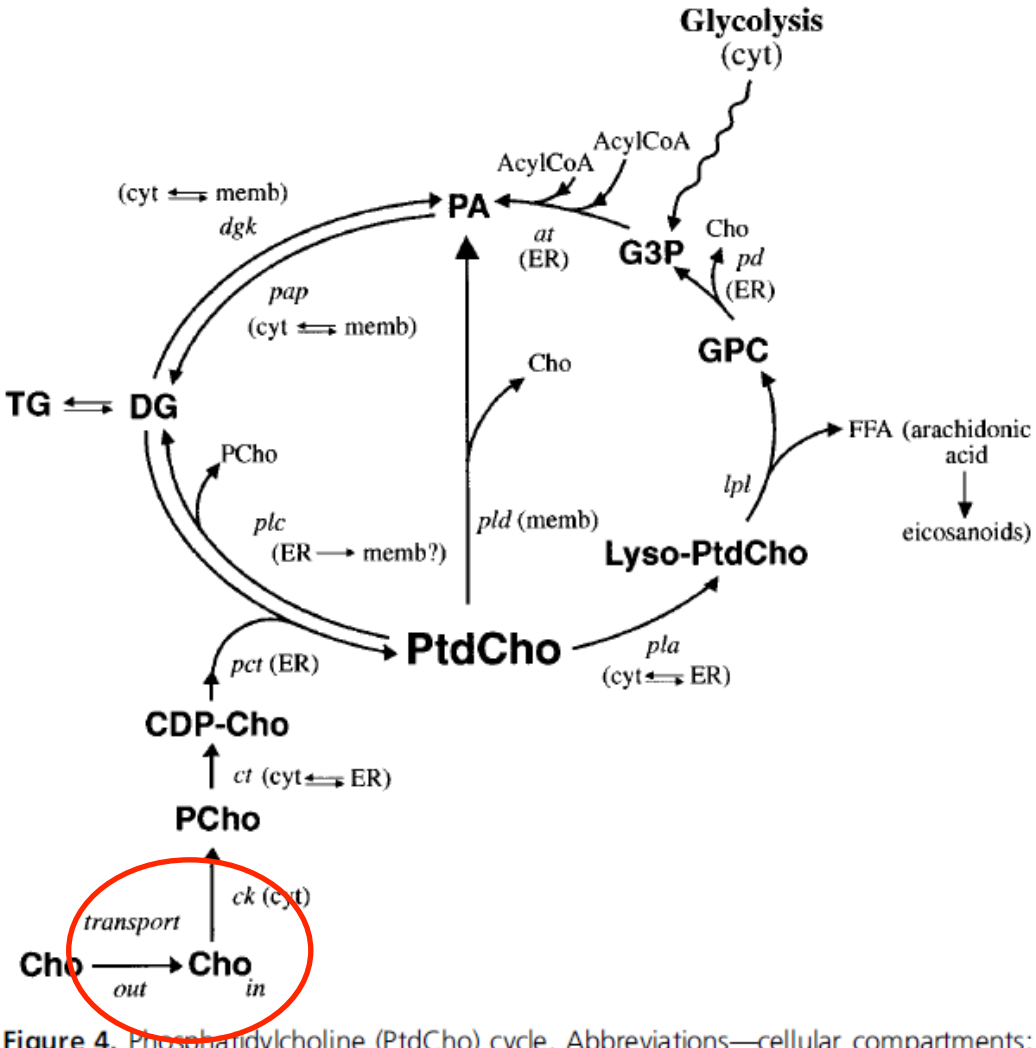


**Figure 4.** Phosphatidylcholine (PtdCho) cycle. Abbreviations—cellular compartments: ER, endoplasmic reticulum; cyt, cytosol; memb, membrane. *Metabolites*: Cho, choline; PCho, phosphocholine; CDP-choline, cytidine diphosphate choline; DG, 1,2-diacylglycerols; PA phosphatidate; Lyso-PtdCho, 1-acyl or 2-acyl phosphatidylcholine; FFA, free fatty acid; GPC, glycerol 3-phosphocholine; G3P, glycerol 3-phosphate; AcylCo-A, acyl coenzyme A. *Enzymes: ck*, choline kinase (EC 2.7.1.32); *ct*, CTP:phosphocholine cytidylyltransferase (EC 2.7.7.15); *pct*, phosphocholine transferase (EC 2.7.8.2); *dgk*, ATP:1,2 diacylglycerol 3-phosphotransferase (EC 2.7.1.107); *pap*, phosphatidate phosphohydrolase (EC 3.1.3.4); *plc*, phospholipase C (EC 3.1.4.3); *pld*, phospholipase D (EC 3.1.4.4); *pla*, $plA_2$ and/or $plA_1$ [ie phospholipase $A_2$ (EC 3.1.1.4) and phospholipase $A_1$ (EC 3.1.1.32)]; *pd*, phosphodiesterase (EC 3.1.4.2); *at*, glycerol-3-phosphate acyltransferases (EC 2.3.1.15 and EC 2.3.1.51); lysophospholipase (EC 3.1.1.5); diacylglycerol acyltransferase (EC 2.3.1.20)

Evaluation de la réponse thérapeutique par TEP à la choline : mise en place et résultats préliminaires (étude PRECHOL)

Julien DUBREUIL

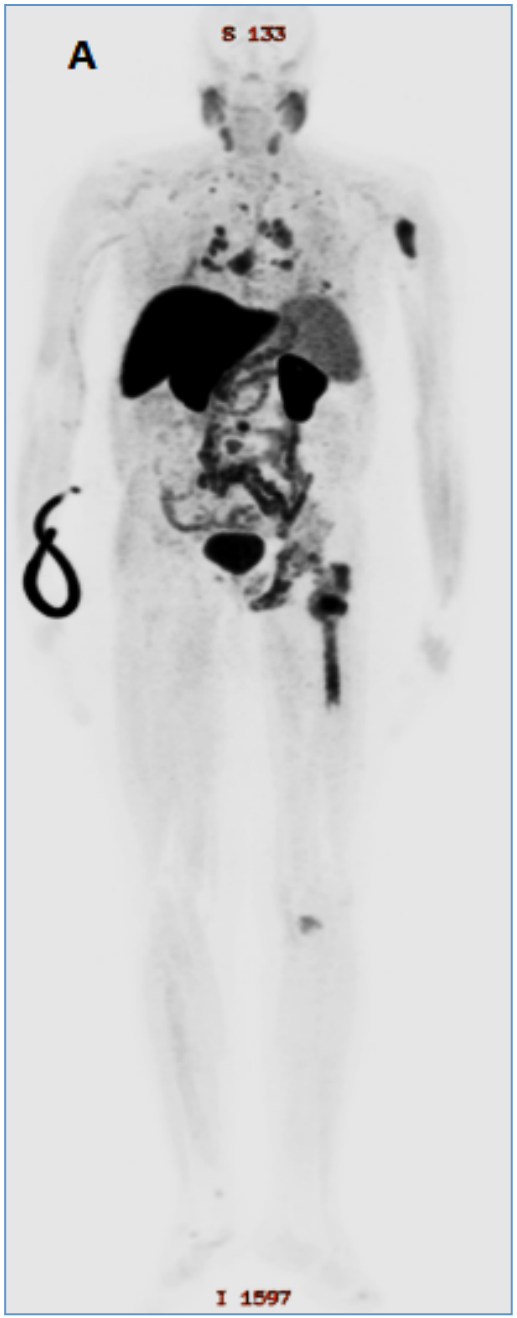


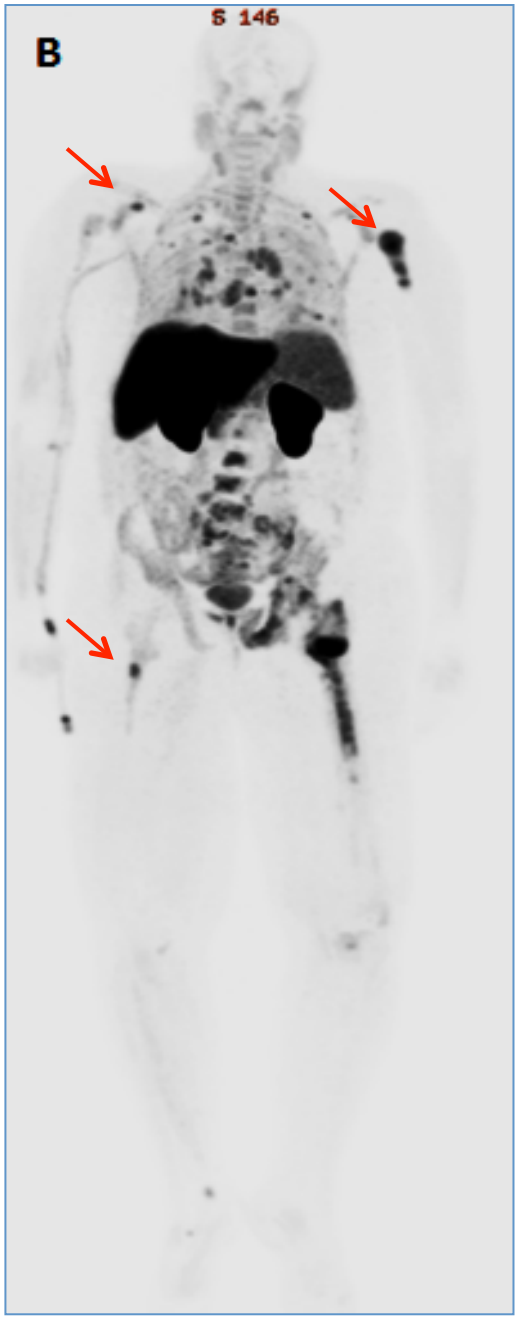


**Figure 1 :** TEP-FCH avant traitement par acétate d'abiratérone **(A)** du patient 5 porteur d'un cancer de la prostate résistant à la castration avec un score de Gleason initial à 7 avec métastases ganglionnaire et osseuse. La TEP-FCH à 6 semaines **(B)** a montré stabilité des lésions existantes (ΔSUVmax = -1.8%) mais l'apparition de nouvelles lésions. Après 12 semaines de traitement, les douleurs, le taux de PSA et la scintigraphie osseuse ont montré une progression selon les critères du PCWG2.

Evaluation de la réponse thérapeutique par TEP à la choline : mise en place et résultats préliminaires (étude PRECHOL)

Julien DUBREUIL

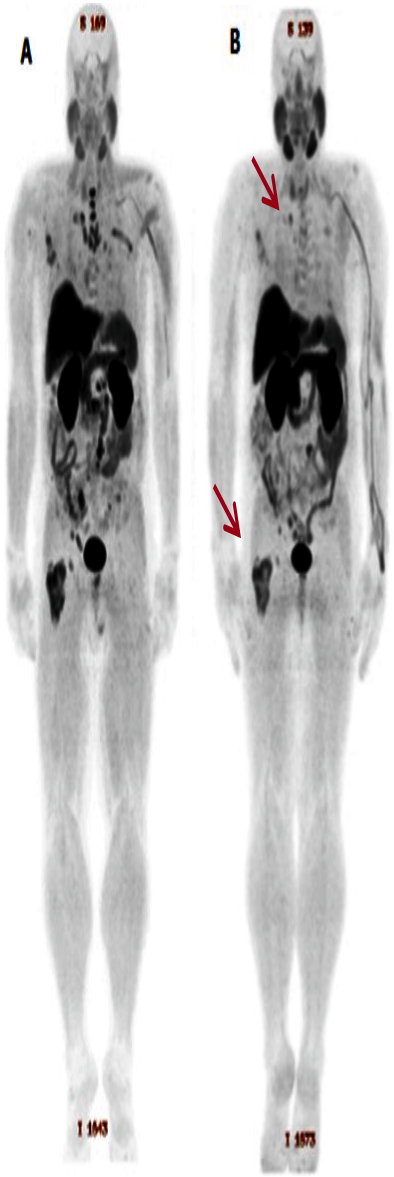


Figure 2 : TEP-FCH avant traitement par acétate d'abiratérone (A) du patient porteur d'un cancer de la prostate métastatique résistant à la castration osseux et ganglionnaires (patient 3). La TEP à 6 semaines (B) est en faveur bonne réponse thérapeutique devant la nette diminution de l'hypermétabolisme des lésions initiales notamment à l'étage thoracique, sans apparition de nouvelles lésions (ΔSUVmax = -59.8%). Après 12 semaines de traitement, les douleurs et la scintigraphie osseuse était stable. L'évolution du taux de PSA était en faveur d'une réponse partielle

# Radiotherapy and PET

- FDG and « MTV »

- other tracers : hypoxia

Journal of Medical Imaging and Radiation Oncology 61 (2017) 124–132

RADIATION ONCOLOGY—ORIGINAL ARTICLE

# Variations in target volume definition and dose to normal tissue using anatomic versus biological imaging ($^{18}$F-FDG-PET) in the treatment of bone metastases: results from a 3-arm randomized phase II trial

Dieter Berwouts,[1,2] Katrien De Wolf,[1] Wilfried De Neve,[1] Luiza AM Olteanu,[1] Bieke Lambert,[2] Bruno Speleers,[1] Ingeborg Goethals,[2] Indira Madani[1] and Piet Ost[1]

**Conclusion:** Positron emitting tomography-information potentially changes the target volume for bone metastases. DPBN between 6 and 10 Gy significantly decreases dose to the normal tissue compared to conventional radiotherapy.

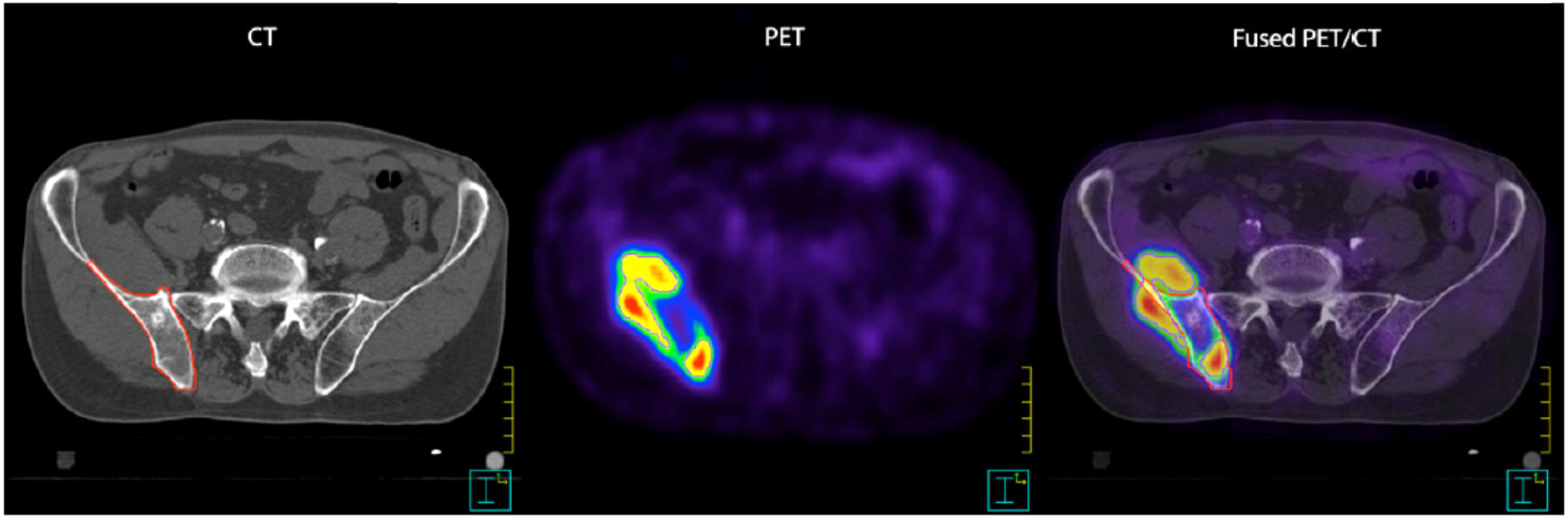


**Fig. 3.** Axial planes of a lung cancer patient who had painful bone metastasis in the right ilium. $SUV_{MAX}$ in the lesion was 13. A relative $SUV_{MAX}$-window was used. Delineated in red is the $GTV_{CT}$ (243 cc); in purple is the $GTV_{PET}$ (43 cc). The right panel shows the CT, the middle panel shows the $^{18}$F-FDG-PET and the left panel shows the fused $^{18}$F-FDG-PET/CT. Jaccard Index and overlap indices for this patient were 0.1 and 0.1, respectively. The $^{18}$F-FDG-PET/CT show minor regions of uptake in the CT-defined bone metastasis, but shows an extra-osseous component.

# Phase II Study of a Radiotherapy Total Dose Increase in Hypoxic Lesions Identified by $^{18}$F-Misonidazole PET/CT in Patients with Non–Small Cell Lung Carcinoma (RTEP5 Study)

Pierre Vera[1], Sébastien Thureau[2], Philippe Chaumet-Riffaud[3], Romain Modzelewski[1], Pierre Bohn[1], Maximilien Vermandel[4], Sébastien Hapdey[1], Amandine Pallardy[5], Marc-André Mahé[6], Marie Lacombe[7], Pierre Boisselier[8], Sophie Guillemard[9], Pierre Olivier[10], Veronique Beckendorf[11], Naji Salem[12], Nathalie Charrier[13], Enrique Chajon[14], Anne Devillers[15], Nicolas Aide[16], Serge Danhier[17], Fabrice Denis[18], Jean-Pierre Muratet[19], Etienne Martin[20], Alina Berriolo Riedinger[21], Helène Kolesnikov-Gauthier[22], Eric Dansin[23], Carole Massabeau[24], Fredéric Courbon[25], Marie-Pierre Farcy Jacquet[26], Pierre-Olivier Kotzki[9,27], Claire Houzard[28], Francoise Mornex[29], Laurent Vervueren[30], Amaury Paumier[31], Philippe Fernandez[32], Mathieu Salaun[33], and Bernard Dubray[2]

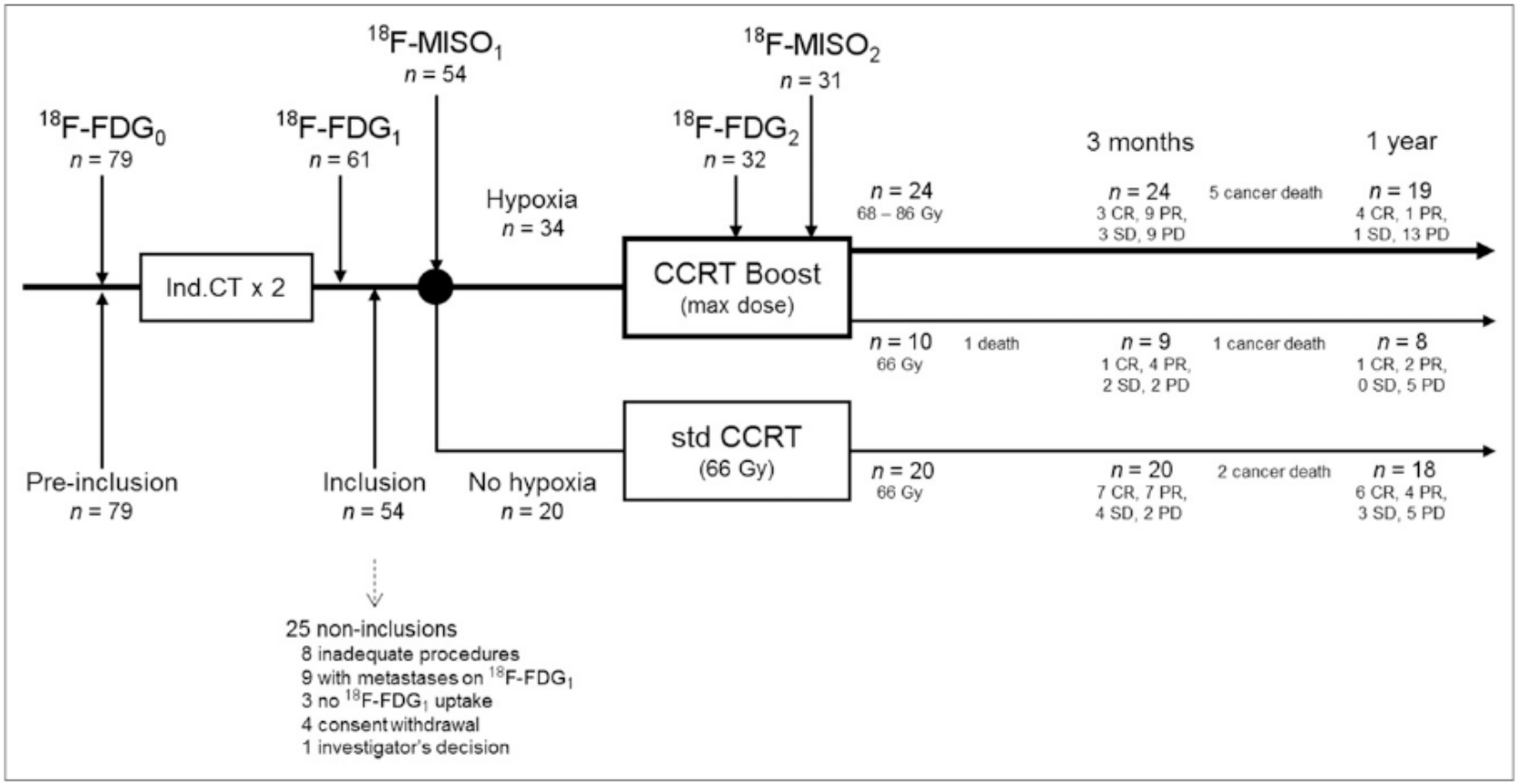


**FIGURE 1.** Study design/study flow. SD = stable disease; PD = progressive disease (RECIST 1.1).

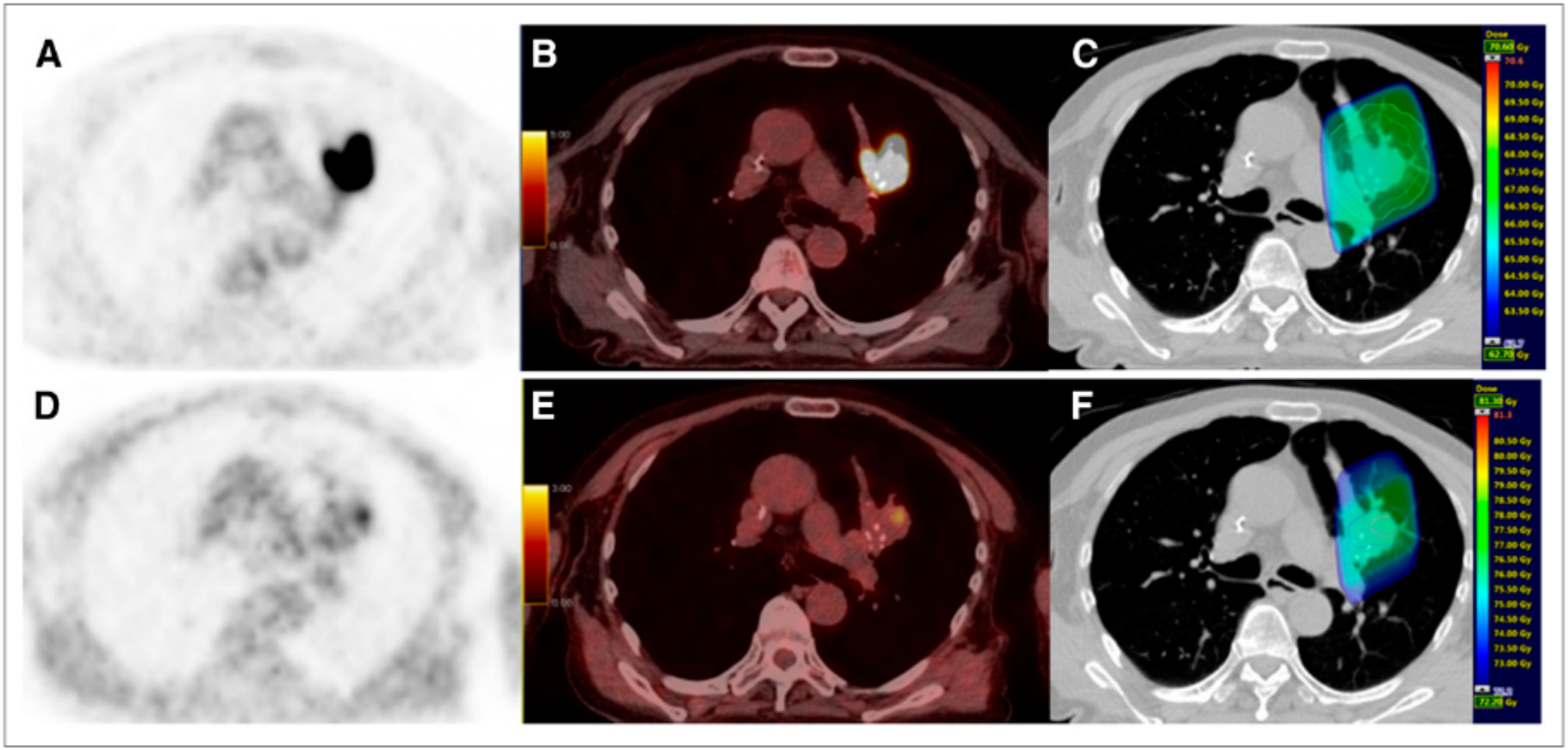


**FIGURE 3.** Example of patient with upper left lung NSCLC: $^{18}$F-FDG (A); $^{18}$F-FDG PET/CT (B); planning radiotherapy based on $^{18}$F-FDG (66 Gy) with $BTV_m$ (gross tumor volume), CTV, and PTV (C); PET $^{18}$F-FMISO (D); $^{18}$F-FMISO PET/CT (E); and boost based on $^{18}$F-FMISO PET (76 Gy) with $BTV_h$ and PTV boost (F).

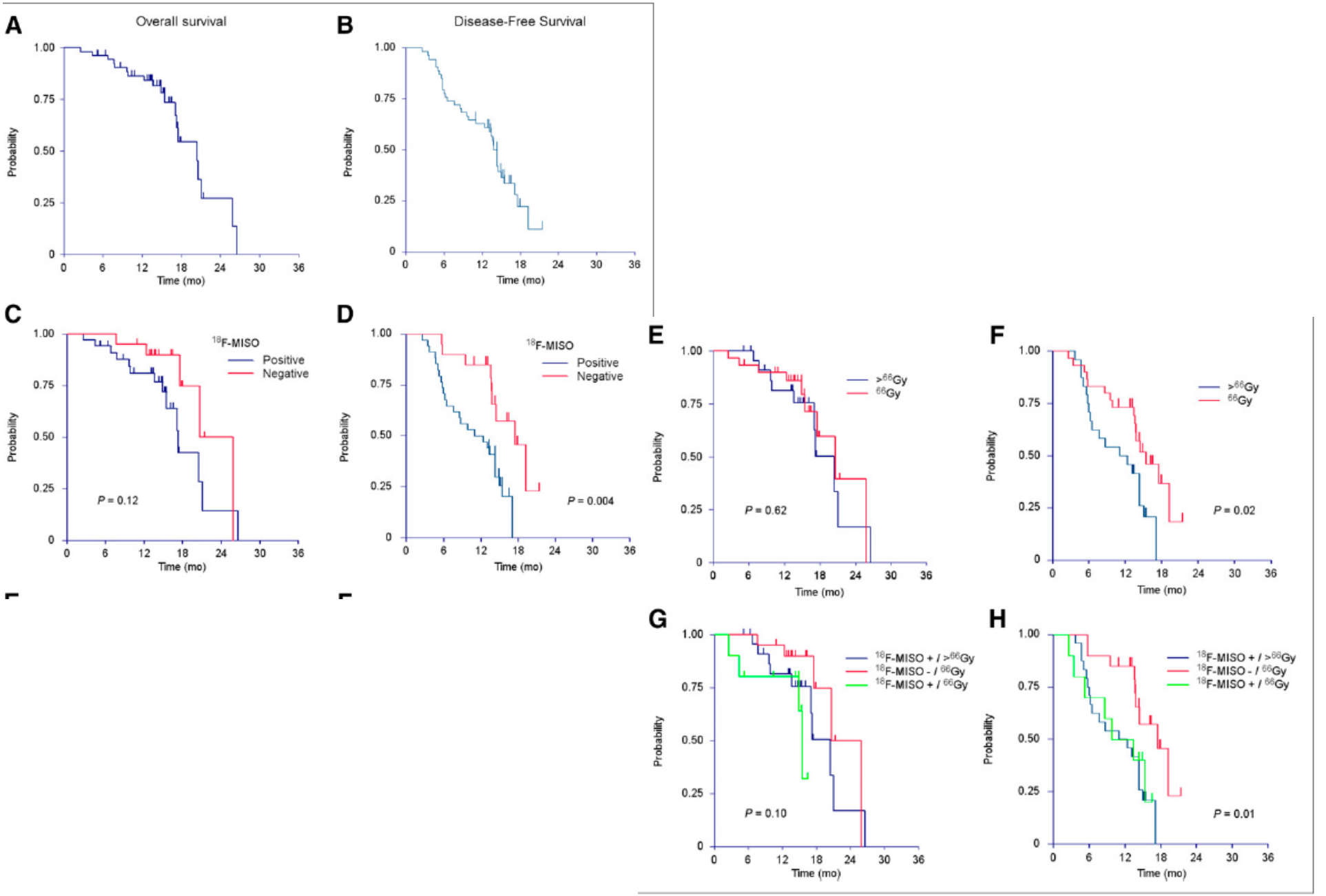


**FIGURE 2.** OS (left) and DFS (right), for entire population (A and B) as well as separation for the $^{18}$F-FMISO PET result (C and D), dose radiation (E and F), and both $^{18}$F-FMISO PET and dose radiation (G and H).

# Conclusions and perspectives

- Tumor metabolism and other cellular processes = biomarkers of tumor progression under and after treatment
- Monitoring tools in nuclear medicine
- Interpretation criteria better and better defined and consensual
- Confirmation by clinical studies of better monitoring and better adaptation of treatments
  - Choice of treatments
  - Early assessment of effectiveness
  - Better diagnosis of remission / residual disease
  - Improved toxicity / efficacy balance and quality of life

# Thank you for your attention

SFMN
Société Française de Médecine Nucléaire
et imagerie moléculaire

Inserm
Institut national
de la santé et de la recherche médic